GRB 080319B: evidence for relativistic turbulence, not internal shocks

Mon. Not. R. Astron. Soc. **395,** 472–489 (2009) doi:10.1111/j.1365-2966.2009.14539.x

GRB 080319B: evidence for relativistic turbulence, not internal shocks

Pawan Kumar[1]★ and Ramesh Narayan[2]

[1]*Astronomy Department, University of Texas, Austin, TX 78712, USA*
[2]*Harvard–Smithsonian Center for Astrophysics, 60 Garden Street, Cambridge, MA 02138, USA*

Accepted 2009 January 21. Received 2009 January 19; in original form 2008 November 29

ABSTRACT

We show that the excellent optical and gamma-ray data available for GRB 080319B rule out the internal shock model for the prompt emission. The data instead point to a model in which the observed radiation was produced close to the deceleration radius ($\sim 10^{17}$ cm) by a turbulent source with random Lorentz factors of $\sim$10 in the comoving frame. The optical radiation was produced by synchrotron emission from relativistic electrons, and the gamma-rays by inverse-Compton scattering of the synchrotron photons. The gamma-ray emission originated both in eddies and in an inter-eddy medium, whereas the optical radiation was mostly from the latter. Therefore, the gamma-ray emission was highly variable whereas the optical was much less variable. The model explains all the observed features in the prompt optical and gamma-ray data of GRB 080319B. We are unable to determine with confidence whether the energy of the explosion was carried outwards primarily by particles (kinetic energy) or magnetic fields. Consequently, we cannot tell whether the turbulent medium was located in the reverse shock (we can rule out the forward shock) or in a Poynting-dominated jet.

Key words: radiation mechanisms: non-thermal – turbulence – gamma-rays: bursts.

1 INTRODUCTION

Two major unsolved questions in the field of gamma-ray bursts (GRBs) are (i) the mechanism by which the energy in relativistic jets is converted to random particle kinetic energy and (ii) the radiation process by which the particle energy is converted to gamma-ray photons.

A number of ideas have been proposed for the conversion of jet energy to particle energy (cf. Thompson 1994; Piran 1999; Mészáros 2002; Lyutikov & Blandford 2003; Piran 2005; Thompson 2006; Zhang 2007). Most popular among these is the so-called internal shock model (Piran, Shemi & Narayan 1993; Katz 1994; Rees & Meszaros 1994), in which different parts of the relativistic GRB jet travel at different speeds. Faster segments collide with slower segments in shocks, and a fraction of the jet kinetic energy is converted to thermal energy. Gamma-rays are then produced by either the synchrotron process or the synchrotron-self-Compton (SSC) process (e.g. Mészáros 2002; Piran 2005; Zhang 2007). Another model is the external shock model (Dermer et al. 1999) in which gamma-rays are produced via the synchrotron process in an external shock driven into the circumstellar medium by the GRB jet. Difficulties with this model have been pointed out by a number of authors (cf. Piran 1999).

The excellent data obtained by the *Swift* and Konus satellites for GRB 080319B – dubbed the 'the naked-eye burst' – have provided a new opportunity to investigate the viability of these models and to understand the fundamental nature of GRBs. We summarize here the main observational properties of this burst (details may be found in Racusin et al. 2008).

GRB 080319B lasted for about 50 s and had a burst fluence in the 20 keV–7 MeV band of $5.7 \pm 0.1 \times 10^{-4}$ erg cm $^{-2}$, which corresponds to an isotropic energy release of $E_\gamma = 1.3 \times 10^{54}$ erg (Golenetskii et al. 2008) for a redshift $z = 0.937$ (Cucchiara & Fox 2008; Vreeswijk et al. 2008). The time-averaged gamma-ray spectrum during the burst had a peak at around 650 keV. The maximum flux at this energy was $\sim$7 mJy, and the time-averaged flux was $\sim$3 mJy. The time-averaged gamma-ray spectrum was measured by Konus–Wind (Racusin et al. 2008) to be $F_\nu \propto \nu^{0.18\pm0.01}$ for photon energies below 650 keV and $F_\nu \propto \nu^{-2.87\pm0.44}$ at higher energies. (The spectrum evolved during the course of the burst, as we discuss in Section 2, and this provides additional information on the radiation process.) In the optical band, at photon energies around 2 eV, the peak flux of GRB 080319B was $V = 5.4$ mag or 20 Jy, and the time-averaged flux was about 10 Jy (Karpov et al. 2008). The optical light curve (LC) varied on a time-scale of about 5 s, while the γ-ray flux varied on time-scales of $\sim$0.5 s.

GRB 080319B has seriously challenged our understanding of GRBs. The problems posed by this burst are described in Kumar & Panaitescu (2008) and discussed in further detail in this paper and in Zou, Piran & Sari (2009). We show that the observations cannot be

★E-mail: pk@astro.as.utexas.edu

explained with any of the standard versions of the internal shock model. We find, however, that a consistent model is possible if we give up the idea of internal shocks and instead postulate that the gamma-ray source is relativistically turbulent (Lyutikov & Blandford 2003; Narayan & Kumar 2009).

We begin in Section 2 by arguing that the radiation in GRB 080319B must have been produced by the SSC mechanism. Following this, we derive in Section 3 the basic equations describing a GRB that radiates via SSC. In Section 4, we combine these equations with the internal shock model and attempt to explain the data on GRB 080319B. We find that no consistent model is possible. In Section 5, we consider a relativistically turbulent model, again with SSC radiation, and show that in this case it is possible to obtain a consistent model of GRB 080319B. We summarize the main conclusions in Section 6. The Appendix discusses the effects of source inhomogeneity on our calculation of the synchrotron self-absorption frequency and the synchrotron and inverse-Compton (IC) fluxes.

2 WHY THE SYNCHROTRON-SELF-COMPTON MODEL?

Racusin et al. (2008; fig. 3) and Wozniak et al. (2008; fig. 4) show that the γ-ray and optical LCs of GRB 080319B have a similar general shape (although the γ-ray LC is a lot more variable than the optical LC). This suggests that the optical and γ-ray radiation were produced by the same region of the source. An independent theoretical argument in support of this conclusion is given in Section 4.1. The radiation mechanisms in the two bands must, however, be different since the optical flux is larger by a factor of $\sim 10^4$ than the γ-ray flux extrapolated to the optical band.

The average spectral properties of GRB 080319B were summarized in Section 1. Racusin et al. (2008; supplementary material – table 1) also reported spectral fits corresponding to three independent time segments of the burst: -2 to 8 s, 12 to 22 s and 26 to 36 s (all times measured with respect to the nominal start time of the burst). The peak of the gamma-ray spectrum evolved from about 750 keV early in the burst to about 550 keV at late times, giving a mean peak energy of 650 keV as mentioned earlier. More interestingly, the spectral slope at energies below the peak evolved with time: $F_\nu \propto \nu^{0.50\pm0.04}$, $\nu^{0.17\pm0.02}$ and $\nu^{0.10\pm0.03}$, during the three time segments. The unusually hard spectrum during the first time segment unambiguously points to an SSC origin for the gamma-ray emission, as we now argue.

The hardest spectrum possible with optically thin synchrotron emission is $F_\nu \propto \nu^{1/3}$. The only way to obtain a harder spectrum is to invoke self-absorption, in which case the spectrum will switch to $F_\nu \propto \nu^2$ below the self-absorption break. However, in order to obtain a synchrotron spectrum with a mean spectral index of 0.5 in the band between 20 and 650 keV, we would need to have the self-absorption break at an energy $\sim$50–100 keV. This has two serious problems. First, it is virtually impossible to push the self-absorption break to such a large energy with any reasonable parameters for the radiating medium.[1] Secondly, a spectral break in which the slope changes from 1/3 to 2 would almost certainly be detectable in the data and would not be consistent with a single power law with a slope of 0.5. Jitter radiation can give rise to a low-energy spectrum $f_\nu \propto \nu$ (Medvedev 2000); however in that case the Compton Y parameter can be shown to be unphysically large – of the order of 10^6 – as described in appendix B of Kumar & McMahon (2008).

A Comptonization model gets around these difficulties. If the gamma-ray emission is produced by Compton-scattering, then any break in the spectrum is not intrinsic to the gamma-rays but merely a reflection of a break in the spectrum of the underlying soft photons. If the soft photons are in the optical-infrared band and are produced by synchrotron emission, then the self-absorption break must be around 0.1 eV, which is perfectly compatible with reasonable model parameters. In addition, although the synchrotron spectrum below the break would be very hard, viz, $F_\nu \propto \nu^2$, the corresponding segment in the up-scattered IC radiation would be softer: $F_\nu \propto \nu$ (Rybicki & Lightman 1979). Thus, the gamma-ray spectrum would break from a slope of 1/3 to 1, which is consistent with the observations, especially when we allow for a smooth rollover from one spectral slope to the other over a range of energies.

Why did the gamma-ray spectral slope below 650 keV switch to $\sim$0.1–0.2 at later times? The likely explanation is that the self-absorption frequency of the synchrotron emission dropped to yet lower energies (in the infrared), and so the break in the gamma-ray band was pushed closer to, or even below, 20 keV.

In this discussion, we have assumed that the soft radiation is produced by the synchrotron process. The alternative is thermal radiation, but this can be ruled out as it requires a Lorentz factor of $\sim 10^8 (\delta t)^{-1} T_5^{-1/2}$ to explain the observed flux of 10 Jy;[2] here δt is the observed variability time (in seconds) of the optical LC and $T_5 = T/10^5$ K is the temperature of the source. The parameter T_5 cannot be much larger than unity since the total energy release would become excessive ($>10^{55}$ erg). A Lorentz factor of 10^8 is not reasonable either. Therefore, a thermal model for the optical emission is ruled out.

[1] For the synchrotron self-absorption frequency to be $\sim$50 keV and the flux at 650 keV to be $\sim$10 mJy, the distance of the emitting region from the centre of the explosion must be less than 10^8 cm. At such a small radius, the medium would be extremely opaque to Thomson scattering and $\gamma + \gamma \rightarrow e^+ + e^-$. Therefore, the emergent radiation would be thermal and no photons with energy $\gtrsim$1 MeV would be able to escape from the source; Konus–Wind detected $\sim$10 MeV photons from GRB 080319B ($e^\pm$ production is suppressed when the bulk Lorentz factor of the source is $\gtrsim 10^2$.). In order to keep the optical depth of the source to Thomson scattering and the Compton Y parameter less than about 1 at this small distance of $\sim 10^8$ cm requires the source Lorentz factor to be larger than $\sim 10^5$ and that is very unlikely.

[2] For a relativistically moving thermal source with a temperature T (in the observer frame) and radius R, the observed flux in the optical band at a frequency $\nu_{\rm op} \sim 5 \times 10^{14}$ Hz is $f_{\rm op} \approx 2\,kT\,(1+z)^4 \nu_{\rm op}^2 R^2/(d_{\rm L}^2 c^2\,\Gamma^2) \approx 2\,kT\,(1+z)^2\,\nu_{\rm op}^2 (\delta t)^2 \Gamma^2 / d_{\rm L}^2$. Therefore, to explain the observed optical flux of 10 Jy, we require $\Gamma \sim 10^8 (\delta t)^{-1} T_5^{-1/2}$.

We thus conclude that the optical photons in GRB 0803019B were produced by the synchrotron mechanism, and the gamma-ray photons were produced by the same relativistic electrons by IC scattering the synchrotron photons. That is, all the observed radiation in GRB 080319B was the result of the SSC process (Section 4 gives a more detailed discussion).

3 SYNCHROTRON AND SSC PROCESSES FOR A RELATIVISTIC TRANSIENT SOURCE: BASIC EQUATIONS

We first determine what properties the source of optical emission in GRB 080319B must have, assuming that the radiation is produced by synchrotron emission (Section 3.1). We then consider the gamma-ray data and describe the additional constraints they provide (Section 3.2). Detailed application to GRB 080319B is discussed in Sections 4 and 5.

3.1 Modelling the prompt optical data

The properties of a synchrotron source can be described by five parameters: B, $N_{\rm e}$, Γ, γ_i and $\tau_{\rm e}$, which are the magnetic field strength, the total number of electrons, the bulk Lorentz factor of the source with respect to the GRB host galaxy, the *typical* electron Lorentz factor in the comoving frame of the source (the electron distribution is $\mathrm{d}n_{\rm e}/\mathrm{d}\gamma \propto \gamma^{-p}$ for $\gamma > \gamma_i$) and the optical depth of the source to Thomson scattering.[3] If the source is at redshift z, the peak frequency ν_i of the synchrotron spectrum and the observed flux f_i at the peak, both as seen by the observer, are given by (Rybicki & Lightman 1979)

$$\nu_i = \frac{\phi_\nu(p) q B \gamma_i^2 \Gamma}{2\pi m_{\rm e} c (1+z)} = (1.15\times10^{-8}\,\mathrm{eV})\,\phi_\nu B \gamma_i^2 \Gamma (1+z)^{-1}, \tag{1}$$

$$f_i = \frac{\sqrt{3}\phi_f(p) q^3 B N_{\rm e} \Gamma (1+z)}{4\pi d_{\rm L}^2 m_{\rm e} c^2} = (0.18\,\mathrm{Jy})\,\phi_f N_{\rm e55} B \Gamma (1+z) d_{\rm L28}^{-2}, \tag{2}$$

where $d_{\rm L}$ is the luminosity distance[4] to the source, and ϕ_ν and ϕ_f are dimensionless constants that depend on the electron energy distribution index p; for $p = 5$ (as suggested by the high-energy spectral index for GRB 080319B), $\phi_\nu = 0.5$ and $\phi_f = 0.7$ (cf. Wijers & Galama 1999[5]). In all subsequent equations we explicitly use these values for the ϕs with the exception that for the most important quantities – such as the total energy and the IC flux – we show the dependence of the results on the ϕs to indicate how uncertainties in ν_i and f_i affect the final result.

Throughout this paper we measure frequencies in eV and fluxes in Jy. All other quantities are in cgs units, but we use the shorthand notation $x_n \equiv x/(10^n\,\mathrm{cgs})$ to scale numerical values, e.g. $R_{15} = R/(10^{15}\,\mathrm{cm})$ is the radius of the radiating shell with respect to the centre of the explosion in units of 10^{15} cm. Using this convention, the source optical depth $\tau_{\rm e}$ and the duration of a pulse in the LC δt (in seconds) are given by

$$\tau_{\rm e} = \frac{\sigma_T N_{\rm e}}{4\pi R^2} = 0.5\frac{N_{\rm e55}}{R_{15}^2} \qquad \text{or} \qquad N_{\rm e55} = 2\tau_{\rm e} R_{15}^2, \tag{3}$$

$$\delta t = \frac{(1+z)R}{2c\Gamma^2} = (1.7\times10^4\,\mathrm{s}) R_{15} \Gamma^{-2} (1+z). \tag{4}$$

Equivalently,

$$\Gamma = 130 (\delta t)^{-1/2} (1+z)^{1/2} R_{15}^{1/2}. \tag{5}$$

We can combine equations (1) and (2) to eliminate B:

$$f_i = \frac{3\times10^7\,\mathrm{Jy}}{\gamma_i^2} \nu_i N_{\rm e55} (1+z)^2 d_{\rm L28}^{-2}, \tag{6}$$

and use equation (3) to replace $N_{\rm e}$ by $\tau_{\rm e}$. The resultant equation is

$$f_i = \frac{4.2\times10^7\,\mathrm{Jy}}{\gamma_i^4} \nu_i Y R_{15}^2 (1+z)^2 d_{\rm L28}^{-2}, \tag{7}$$

or

$$\gamma_i = 81 f_i^{-1/4} \nu_i^{1/4} Y^{1/4} R_{15}^{1/2} (1+z)^{1/2} d_{\rm L28}^{-1/2}. \tag{8}$$

Here, we have defined the quantity

$$Y \equiv \gamma_i^2 \tau_{\rm e}, \tag{9}$$

[3] Technically, the electron index p is a sixth parameter, but since it can be estimated directly from the high-energy slope of the gamma-ray spectrum we do not count it.

[4] The factor (1+z) in the numerator of the expression for flux in equation (2) is due to the fact that the luminosity distance refers to the bolometric flux whereas we are considering the flux per unit frequency.

[5] $\phi_\nu = 1.5 x_{\rm p}$ and $\phi_f = \phi_{\rm p}$ in the notation of Wijers & Galama.

which is closely related to, but smaller by a factor of 2–3 than, the Compton Y parameter for GRB 080319B (the difference depends on the electron distribution function). Substituting equations (5) and (8) back into equation (1), we find

$$B = (205G)(\delta t)^{1/2}\nu_i^{1/2} f_i^{1/2} Y^{-1/2} R_{15}^{-3/2}(1+z)^{-1/2} d_{\rm L28}, \tag{10}$$

while equations (3) and (8) yield

$$N_{\rm e55} = 2.9\times10^{-4}\nu_i^{-1/2} f_i^{1/2} Y^{1/2} R_{15}(1+z)^{-1} d_{\rm L28}. \tag{11}$$

Equations (3), (5), (8), (10) and (11) are solutions for the five basic physical parameters of the synchrotron source in terms of the observed variability time δt and four unknown quantities: the source radius R_{15}, the Compton parameter Y, the peak energy of the synchrotron spectrum ν_i and the synchrotron flux at the peak f_i. The last two quantities are not independent – they are constrained by the observed optical flux $f_{\rm op}$(=10 Jy in the case of GRB 080319B) at 2 eV. Depending on whether the synchrotron peak frequency ν_i is below or above 2 eV, we obtain the following constraint:

$$f_{\rm op} = \begin{cases} f_i(2/\nu_i)^{1/3}, & \nu_i > 2, \\ f_i(\nu_i/2)^{p/2}, & \nu_i < 2, \end{cases} \tag{12}$$

where we have used standard results for the spectral slope below and above the synchrotron peak, assuming for the latter that the cooling frequency is close to ν_i, as suggested by the spectrum of GRB 080319B;[6] for other bursts, where the cooling break is substantially above the synchrotron peak, the equations in this paper can be easily modified by replacing p with $(p-1)$.

Another constraint is provided by the synchrotron self-absorption frequency $\nu_{\rm a}$, which can be estimated by equating the synchrotron flux at $\nu_{\rm a}$ to the blackbody flux in the Rayleigh–Jeans limit. Assuming that the electrons that dominate at $\nu_{\rm a}$ have Lorentz factor γ_i, we obtain

$$\frac{2\pi\nu_{\rm a}'^2}{c^2} m_{\rm e}c^2\gamma_i = f'(\nu_{\rm a}') = \frac{f_i}{\Gamma}\frac{d_{\rm L}^2}{(1+z)R^2}\left(\frac{\nu_{\rm a}'}{\nu_i'}\right)^{1/3}, \tag{13}$$

where primes refer to quantities in the source comoving frame. To convert to the observer frame, we use

$$\nu_{\rm a} \equiv \nu_{\rm a}'\Gamma/(1+z). \tag{14}$$

Combining the above two equations, we find

$$\nu_{\rm a} = 1.9 f_i^{3/5}\nu_i^{-1/5}\Gamma^{3/5}\gamma_i^{-3/5} R_{15}^{-6/5}(1+z)^{-9/5} d_{\rm L28}^{6/5}. \tag{15}$$

As before, all frequencies are in eV and fluxes in Jy. Substituting for Γ and γ_i from equations (5) and (8) results in

$$\nu_{\rm a} = 2.5 f_i^{3/4}\nu_i^{-7/20}(\delta t)^{-3/10} R_{15}^{-6/5} Y^{-3/20}(1+z)^{-9/5} d_{\rm L28}^{3/2}. \tag{16}$$

As we discuss in Section 3.2, we can estimate from the gamma-ray data the ratio η of the synchrotron frequency ν_i to the self-absorption frequency $\nu_{\rm a}$:

$$\eta \equiv \nu_i/\nu_{\rm a}. \tag{17}$$

Therefore, this is a third observational constraint on the source properties.

To summarize, the source of optical emission is described by means of five parameters. The pulse duration δt, the optical flux $f_{\rm op}$ and the frequency ratio η (equation 17) give three constraints. The solution space is thus reduced to a two-dimensional surface. Additional constraints are obtained from the gamma-ray data, as we discuss next.

3.2 Gamma-ray emission via the inverse-Compton process

We assume that the gamma-rays are produced by IC scattering of synchrotron photons. The peak frequency $\nu_{\rm ic}$ of the IC spectrum and the flux $f_{\rm ic}$ at the peak are related to ν_i and f_i as follows:

$$\nu_{\rm ic} \approx 3\gamma_i^2\nu_i, \qquad f_{\rm ic} \approx 3\tau_{\rm e} f_i = 3Y\gamma_i^{-2} f_i, \tag{18}$$

where a multiplicative factor of 3 in the expression for $f_{\rm ic}$ takes into account the ratio of solid-angle-integrated specific intensity inside the source and the flux just outside the shell (in the source comoving frame). Substituting for γ_i from equation (8),

$$\nu_{\rm ic6} = 1.9\times10^{-2} f_i^{-1/2}\nu_i^{3/2} Y^{1/2} R_{15}(1+z) d_{\rm L28}^{-1}, \tag{19}$$

$$f_{\rm ic-3} = 0.47 f_i^{3/2}\nu_i^{-1/2} Y^{1/2} R_{15}^{-1}(1+z)^{-1} d_{\rm L28}, \tag{20}$$

where $\nu_{\rm ic6} = \nu_{\rm ic}/(10^6\ {\rm eV})$ and $f_{\rm ic-3} = f_{\rm ic}/(10^{-3}\ {\rm Jy})$.

Using equation (19) for $\nu_{\rm ic}$, we determine the synchrotron peak flux,

$$f_i = 3.8\times10^{-4}\nu_{\rm ic6}^{-2}\nu_i^3 R_{15}^2 Y(1+z)^2 d_{\rm L28}^{-2}, \tag{21}$$

[6] The spectrum of GRB 080319B peaked at 650 keV and contained no other break between 20 keV and 7 MeV. Since the cooling frequency cannot be smaller than 650 keV since the spectrum varies as $\nu^{0.2}$ below the peak, it must be either larger than 7 MeV or close to 650 keV. The former possibility is unlikely since it corresponds to a radiatively inefficient system and would increase the energy requirement of an already extreme burst.

and substituting this into equation (16) we obtain ν_i:

$$\nu_i = 1.2 \times 10^2 \eta^{-10/9} \nu_{\rm ic6}^{5/3} (\delta t)^{1/3} R_{15}^{-1/3} Y^{-2/3} (1+z)^{1/3}. \tag{22}$$

Eliminating ν_i from equation (21) by using equation (22), we find

$$f_i = 6.6 \times 10^2 \eta^{-10/3} \nu_{\rm ic6}^3 \delta t\, R_{15} Y^{-1} (1+z)^3 d_{\rm L28}^{-2}. \tag{23}$$

Substituting for ν_i and f_i from equations (22) and (23) into equation (12) for the optical flux, we obtain

$$f_{\rm op} = \begin{cases} 166\, \eta^{-\frac{80}{27}} \nu_{\rm ic6}^{\frac{22}{9}} (\delta t)^{\frac{8}{9}} R_{15}^{\frac{10}{9}} Y^{-\frac{7}{9}} (1+z)^{\frac{26}{9}} d_{\rm L28}^{-2}, & \nu_i > 2, \\ 922 \times 8.7^p\, \eta^{-\frac{5(p+6)}{9}} \nu_{\rm ic6}^{\frac{5p+18}{6}} (\delta t)^{\frac{p+6}{6}} R_{15}^{\frac{6-p}{6}} Y^{-\frac{p+3}{3}} (1+z)^{\frac{p+18}{6}} d_{\rm L28}^{-2} (\phi_\nu/\phi_f)^{\frac{3+p}{3}}, & \nu_i < 2. \end{cases} \tag{24}$$

We use the optical flux to eliminate one more unknown variable, Y,

$$Y = \begin{cases} 714\, \eta^{-\frac{80}{21}} f_{\rm op}^{-\frac{9}{7}} \nu_{\rm ic6}^{\frac{22}{7}} (\delta t)^{\frac{8}{7}} R_{15}^{\frac{10}{7}} (1+z)^{\frac{26}{7}} d_{\rm L28}^{-\frac{18}{7}}, & \nu_i > 2, \\ 471 \times 1.4^{\frac{3}{p+3}}\, \eta^{-\frac{5(p+6)}{3(p+3)}} f_{\rm op}^{-\frac{3}{p+3}} \nu_{\rm ic6}^{\frac{5p+18}{2p+6}} (\delta t)^{\frac{p+6}{2p+6}} R_{15}^{\frac{6-p}{2p+6}} (1+z)^{\frac{p+18}{2p+6}} d_{\rm L28}^{-\frac{6}{p+3}}, & \nu_i < 2. \end{cases} \tag{25}$$

We are now in a position to express all quantities in terms of four observables, viz, the pulse duration δt, the optical flux $f_{\rm op}$, the dimensionless self-absorption frequency η and the peak frequency of the gamma-ray spectrum $\nu_{\rm ic}$, plus one unknown parameter R_{15}.

The peak frequency of the synchrotron spectrum is obtained from equations (22) and (25):

$$\nu_i = \begin{cases} 1.5\, \eta^{\frac{10}{7}} f_{\rm op}^{\frac{6}{7}} \nu_{\rm ic6}^{-\frac{3}{7}} (\delta t)^{-\frac{3}{7}} R_{15}^{-\frac{9}{7}} (1+z)^{-\frac{15}{7}} d_{\rm L28}^{\frac{12}{7}}, & \nu_i > 2, \\ 2 \times 1.4^{-\frac{2}{p+3}}\, \eta^{\frac{10}{3(p+3)}} f_{\rm op}^{\frac{2}{p+3}} \nu_{\rm ic6}^{-\frac{1}{p+3}} (\delta t)^{-\frac{1}{p+3}} R_{15}^{-\frac{3}{p+3}} (1+z)^{-\frac{5}{p+3}} d_{\rm L28}^{\frac{4}{p+3}}, & \nu_i < 2. \end{cases} \tag{26}$$

Let us define the transition radius $R_{\rm tr}$ as that value of R for which $\nu_i = 2$ eV. From equation (26), we find

$$R_{\rm tr,15} = 0.8 \eta^{\frac{10}{9}} f_{\rm op}^{\frac{2}{3}} \nu_{\rm ic6}^{-\frac{1}{3}} (\delta t)^{-\frac{1}{3}} (1+z)^{-\frac{5}{3}} d_{\rm L28}^{\frac{4}{3}}. \tag{27}$$

Note that, for $R > R_{\rm tr}$, $\nu_i < 2$ eV and vice versa.

The flux at the peak of the synchrotron spectrum is obtained from equations (23) and (25):

$$f_i = \begin{cases} 0.92\, \eta^{\frac{10}{21}} f_{\rm op}^{\frac{9}{7}} \nu_{\rm ic6}^{-\frac{1}{7}} (\delta t)^{-\frac{1}{7}} R_{15}^{-\frac{3}{7}} (1+z)^{-\frac{5}{7}} d_{\rm L28}^{\frac{4}{7}}, & R < R_{\rm tr}, \\ 1.4^{\frac{p}{p+3}}\, \eta^{-\frac{5p}{3(p+3)}} f_{\rm op}^{\frac{3}{p+3}} \nu_{\rm ic6}^{\frac{p}{2p+6}} (\delta t)^{\frac{p}{2p+6}} R_{15}^{\frac{3p}{2p+6}} (1+z)^{\frac{5p}{2p+6}} d_{\rm L28}^{-\frac{2p}{p+3}}, & R > R_{\rm tr}, \end{cases} \tag{28}$$

and the peak gamma-ray flux is obtained from equations (20), (25), (26) and (28):

$$f_{\rm ic-3} = \frac{\phi_\nu}{\phi_f} \begin{cases} 12.3\, \eta^{-\frac{40}{21}} f_{\rm op}^{\frac{6}{7}} \nu_{\rm ic6}^{\frac{11}{7}} (\delta t)^{\frac{4}{7}} R_{15}^{-\frac{2}{7}} (1+z)^{\frac{6}{7}} d_{\rm L28}^{-\frac{2}{7}}, & R < R_{\rm tr}, \\ 8.4 \times 1.4^{\frac{2p+4}{p+3}}\, \eta^{-\frac{10(p+2)}{3(p+3)}} f_{\rm op}^{\frac{2}{p+3}} \nu_{\rm ic6}^{\frac{2p+5}{p+3}} (\delta t)^{\frac{p+2}{p+3}} R_{15}^{\frac{p}{p+3}} (1+z)^{\frac{3p+4}{p+3}} d_{\rm L28}^{-\frac{2p+2}{p+3}}, & R > R_{\rm tr}. \end{cases} \tag{29}$$

Using equations (25), (26) and (28) to substitute for Y, ν_i and f_i, equations (8), (10) and (11) give

$$\gamma_i = \begin{cases} 555\, \eta^{-\frac{5}{7}} f_{\rm op}^{-\frac{3}{7}} \nu_{\rm ic6}^{\frac{5}{7}} (\delta t)^{\frac{3}{14}} R_{15}^{\frac{9}{14}} (1+z)^{\frac{15}{14}} d_{\rm L28}^{-\frac{6}{7}}, & R < R_{\rm tr}, \\ 527\, \eta^{-\frac{5}{3(p+3)}} f_{\rm op}^{-\frac{1}{p+3}} \nu_{\rm ic6}^{\frac{p+4}{2p+6}} (\delta t)^{\frac{1}{2p+6}} R_{15}^{\frac{3}{2p+6}} (1+z)^{\frac{5}{2p+6}} d_{\rm L28}^{-\frac{4}{2(p+3)}}, & R > R_{\rm tr}, \end{cases} \tag{30}$$

$$B = \phi_\nu^{-1} \begin{cases} 4.5{\rm G}\, \eta^{\frac{20}{7}} f_{\rm op}^{\frac{12}{7}} \nu_{\rm ic6}^{-\frac{13}{7}} (\delta t)^{-\frac{5}{14}} R_{15}^{-\frac{43}{14}} (1+z)^{-\frac{53}{14}} d_{\rm L28}^{\frac{24}{7}}, & R < R_{\rm tr}, \\ 6.7{\rm G}\, \eta^{\frac{20}{3(p+3)}} f_{\rm op}^{\frac{4}{p+3}} \nu_{\rm ic6}^{-\frac{p+5}{p+3}} (\delta t)^{\frac{p-1}{2p+6}} R_{15}^{-\frac{p+15}{2p+6}} (1+z)^{-\frac{17-p}{2p+6}} d_{\rm L28}^{\frac{8}{p+3}}, & R > R_{\rm tr}, \end{cases} \tag{31}$$

$$N_{\rm e55} = \begin{cases} 6.1 \times 10^{-3}\, \eta^{-\frac{50}{21}} f_{\rm op}^{-\frac{3}{7}} \nu_{\rm ic6}^{\frac{12}{7}} (\delta t)^{\frac{5}{7}} R_{15}^{\frac{15}{7}} (1+z)^{\frac{11}{7}} d_{\rm L28}^{-\frac{6}{7}}, & R < R_{\rm tr}, \\ 5.9 \times 10^{-3}\, \eta^{-\frac{5(p+4)}{3(p+3)}} f_{\rm op}^{-\frac{1}{p+3}} \nu_{\rm ic6}^{\frac{3p+10}{2p+6}} (\delta t)^{\frac{p+4}{2p+6}} R_{15}^{\frac{3p+12}{2p+6}} (1+z)^{\frac{p+8}{2p+6}} d_{\rm L28}^{-\frac{2}{p+3}}, & R > R_{\rm tr}. \end{cases} \tag{32}$$

The energy in the magnetic field as measured in the GRB host galaxy rest frame is $E_B = B^2 R^3/2$. Using equation (31), this can be shown to be

$$E_B = \begin{cases} 1.2 \times 10^{46}\ {\rm erg}\ \eta^{\frac{40}{7}} f_{\rm op}^{\frac{24}{7}} \nu_{\rm ic6}^{-\frac{26}{7}} (\delta t)^{-\frac{5}{7}} R_{15}^{-\frac{22}{7}} (1+z)^{-\frac{53}{7}} d_{\rm L28}^{\frac{48}{7}} \phi_\nu^{-2}, & R < R_{\rm tr}, \\ 2 \times 10^{46}\ {\rm erg}\ \eta^{\frac{40}{3(p+3)}} f_{\rm op}^{\frac{8}{p+3}} \nu_{\rm ic6}^{-\frac{2p+10}{p+3}} (\delta t)^{\frac{p-1}{p+3}} R_{15}^{\frac{2p-6}{p+3}} (1+z)^{-\frac{17-p}{p+3}} d_{\rm L28}^{\frac{16}{p+3}} \phi_\nu^{-2}, & R > R_{\rm tr}. \end{cases} \tag{33}$$

The energy in the charged particles ($e^{\pm}$) that produce the optical and gamma-ray emission is $E_{\rm e} = N_{\rm e} \gamma_i \Gamma m_{\rm e} c^2$. From equations (5), (30) and (32), this is

$$E_{\rm e} = \begin{cases} 4 \times 10^{51}\ {\rm erg}\ \eta^{-\frac{65}{21}} f_{\rm op}^{-\frac{6}{7}} \nu_{\rm ic6}^{\frac{17}{7}} (\delta t)^{\frac{3}{7}} R_{15}^{\frac{23}{7}} (1+z)^{\frac{22}{7}} d_{\rm L28}^{-\frac{12}{7}} (\phi_\nu/\phi_f)^{\frac{1}{2}}, & R < R_{\rm tr}, \\ 3 \times 10^{51}\ {\rm erg}\ \eta^{-\frac{(5p+25)}{3(p+3)}} f_{\rm op}^{-\frac{2}{p+3}} \nu_{\rm ic6}^{\frac{2p+7}{p+3}} (\delta t)^{\frac{1}{p+3}} R_{15}^{\frac{2p+9}{p+3}} (1+z)^{\frac{p+8}{p+3}} d_{\rm L28}^{-\frac{4}{p+3}} (\phi_\nu/\phi_f)^{\frac{1}{2}}, & R > R_{\rm tr}. \end{cases} \tag{34}$$

We should also consider the energy in the protons arising from the bulk relativistic motion of the shell. However, to estimate this quantity we need to make some assumption regarding the composition of the fluid in the shell, whether it is primarily an e^+e^- plasma or a p^+e^- plasma.

In the former case, the energy in protons is negligible, while in the latter case the energy is $E_{\rm p} = N_{\rm e}\Gamma m_{\rm p}c^2 \sim$ few $\times E_{\rm e}$ (taking γ_i of the order of a few hundred).

In the observer frame, the synchrotron cooling time $t_{\rm syn}$ is

$$t_{\rm syn} = (7.7\times10^8\,s)(1+z)\Gamma^{-1}B^{-2}\gamma_i^{-1}, \tag{35}$$

which, using equations (5), (30) and (31), can be written as

$$t_{\rm syn} = \frac{\phi_\nu^{5/2}}{\phi_f^{1/2}} \begin{cases} (620\,{\rm s})\ \eta^{-5} f_{\rm op}^{-3} \nu_{\rm ic6}^3(\delta t) R_{15}^5 (1+z)^7 d_{\rm L28}^{-6}, & R < R_{\rm tr}, \\ (295\,{\rm s})\ \eta^{-\frac{35}{3(p+3)}} f_{\rm op}^{-\frac{7}{p+3}} \nu_{\rm ic6}^{\frac{3p+16}{2p+6}} (\delta t)^{\frac{4-p}{2p+6}} R_{15}^{\frac{p+24}{2p+6}} (1+z)^{\frac{32-p}{2p+6}} d_{\rm L28}^{-\frac{14}{p+3}}, & R > R_{\rm tr}. \end{cases} \tag{36}$$

In addition to the loss of energy via synchrotron radiation, electrons also lose energy through IC scattering of the local radiation field. We calculate the photon energy density in the source rest frame from the observed bolometric luminosity $L_{\rm obs}$, and use this to estimate the IC cooling time $t_{\rm ic}$ in the observer frame:

$$t_{\rm ic} = \frac{4\pi R^2 \Gamma (1+z) m_{\rm e} c^2}{L_{\rm obs}\gamma_i \sigma_T} = (0.2{\rm s}) L_{\rm obs,52}^{-1} (\delta t)^{-1/2} R_{15}^{5/2} (1+z)^{3/2} \gamma_i^{-1}. \tag{37}$$

Strictly speaking, we do not know the true bolometric luminosity, so the above estimate of $t_{\rm ic}$ is an upper limit to the actual IC cooling time. Using equation (30), we can rewrite $t_{\rm ic}$ in the following more useful form:

$$t_{\rm ic} = \frac{\phi_\nu^{\frac{1}{2}}}{\phi_f^{\frac{1}{2}}} \begin{cases} \frac{4\times10^{-4}\,{\rm s}}{L_{\rm obs,52}}\ \eta^{\frac{5}{7}} f_{\rm op}^{\frac{3}{7}} \nu_{\rm ic6}^{-\frac{5}{7}} (\delta t)^{-\frac{5}{7}} R_{15}^{\frac{13}{7}} (1+z)^{\frac{3}{7}} d_{\rm L28}^{\frac{6}{7}}, & R < R_{\rm tr}, \\ \frac{4.5\times10^{-4}\,{\rm s}}{L_{\rm obs,52}}\ \eta^{\frac{5}{3(p+3)}} f_{\rm op}^{\frac{1}{p+3}} \nu_{\rm ic6}^{-\frac{p+4}{2p+6}} (\delta t)^{-\frac{p+4}{2p+6}} R_{15}^{\frac{5p+12}{2p+6}} (1+z)^{\frac{3p+4}{2p+6}} d_{\rm L28}^{\frac{2}{p+3}}, & R > R_{\rm tr}. \end{cases} \tag{38}$$

All the results obtained so far are general and could be applied to any GRB that has the required data. We now consider the implications for the naked-eye burst GRB 080319B.

4 APPLICATION TO GRB 080319B: RULING OUT THE INTERNAL SHOCK MODEL

The relevant observational parameters for GRB 080319B are $z = 0.94$, $d_{\rm L28} = 1.9$, $f_{\rm op} = 10$ Jy, $\nu_{\rm ic6} = 0.665$, $p = 5$ and $\delta t \sim 1$ s (from the gamma-ray variability). Moreover, we estimate that[7] the time-averaged $\eta \equiv \nu_i/\nu_{\rm a}$ for this burst was about 25 (because $f_\nu \propto \nu^{0.18\pm0.01}$ between 20 and 650 keV), whereas the initial value of η was $\sim$10 as $f_\nu \propto \nu^{0.5\pm0.04}$ during the first 8 s. Scaling all quantities to these values, the transition radius $R_{\rm tr}$ becomes

$$R_{\rm tr,16} = 12\eta_{1.4}^{\frac{10}{9}} f_{\rm op,1}^{\frac{2}{3}} \nu_{\rm ic5.8}^{-\frac{1}{3}} (\delta t)^{-\frac{1}{3}}. \tag{39}$$

If $R_{16} > R_{\rm tr,16}$, then $\nu_i < 2$ eV and the optical band is in the steep decaying part of the synchrotron spectrum, above the synchrotron peak. If $R_{16} < R_{\rm tr,16}$, then the synchrotron peak is above 2 eV, and the optical band is in the $F_\nu \propto \nu^{1/3}$ part of the synchrotron spectrum. Since the prompt optical emission in GRB 080319B was exceptionally bright, it is likely that the peak of the synchrotron spectrum was fairly close to the optical band. This suggests that R_{16} must be within a factor of a few of $R_{\rm tr,16}$. According to equation (39), $R_{\rm tr} \sim 10^{17}$ cm, which is orders of magnitude larger than the radius at which internal shocks are expected. In fact, it is comparable to the deceleration radius of the jet.

From the results described in Section 3, we obtain the following numerical results for the relevant parameters in GRB 080319B:

$$\Gamma = 572(\delta t)^{-1/2} R_{16}^{1/2}, \tag{40}$$

$$\gamma_i = \begin{cases} 77\,\eta_{1.4}^{-\frac{5}{7}} f_{\rm op,1}^{-\frac{3}{7}} \nu_{\rm ic5.8}^{\frac{5}{7}} (\delta t)^{\frac{3}{14}} R_{16}^{\frac{9}{14}}, & R < R_{\rm tr}, \\ 251\,\eta_{1.4}^{-\frac{5}{24}} f_{\rm op,1}^{-\frac{1}{8}} \nu_{\rm ic5.8}^{\frac{9}{16}} (\delta t)^{\frac{1}{16}} R_{16}^{\frac{3}{16}}, & R > R_{\rm tr}, \end{cases} \tag{41}$$

$$N_{\rm e} = \begin{cases} 1.1\times10^{51}\ \eta_{1.4}^{-\frac{50}{21}} f_{\rm op,1}^{-\frac{3}{7}} \nu_{\rm ic5.8}^{\frac{12}{7}} (\delta t)^{\frac{5}{7}} R_{16}^{\frac{15}{7}}, & R < R_{\rm tr}, \\ 3.4\times10^{51}\ \eta_{1.4}^{-\frac{15}{8}} f_{\rm op,1}^{-\frac{1}{8}} \nu_{\rm ic5.8}^{\frac{25}{16}} (\delta t)^{\frac{9}{16}} R_{16}^{\frac{27}{16}}, & R > R_{\rm tr}, \end{cases} \tag{42}$$

$$Y = \begin{cases} 2.5\times10^{-3}\,\eta_{1.4}^{-\frac{80}{21}} f_{\rm op,1}^{-\frac{9}{7}} \nu_{\rm ic5.8}^{\frac{22}{7}} (\delta t)^{\frac{8}{7}} R_{16}^{\frac{10}{7}}, & R < R_{\rm tr}, \\ 7.5\times10^{-2}\,\eta_{1.4}^{-\frac{55}{24}} f_{\rm op,1}^{-\frac{3}{8}} \nu_{\rm ic5.8}^{\frac{43}{16}} (\delta t)^{\frac{11}{16}} R_{16}^{\frac{1}{16}}, & R > R_{\rm tr}. \end{cases} \tag{43}$$

$$E_B = \begin{cases} (2\times10^{55}\ {\rm erg})\ \eta_{1.4}^{\frac{40}{7}} f_{\rm op,1}^{\frac{24}{7}} \nu_{\rm ic5.8}^{-\frac{26}{7}} (\delta t)^{-\frac{5}{7}} R_{16}^{-\frac{22}{7}}, & R < R_{\rm tr}, \\ (2.3\times10^{51}\ {\rm erg})\ \eta_{1.4}^{\frac{5}{2}} f_{\rm op,1} \nu_{\rm ic5.8}^{-\frac{5}{2}} (\delta t)^{\frac{1}{2}} R_{16}^{\frac{1}{2}}, & R > R_{\rm tr}, \end{cases} \tag{44}$$

[7] The spectral indices are obtained by fitting the data with the band function, which gives the asymptotic value for the low- and high-energy index. It should be noted that the IC spectrum below $\sim 2\gamma_i^2\nu_{\rm a}$ is $f_\nu \propto \nu$, and between this frequency and the peak of νf_ν at $3\gamma_i^2\nu_i$ the spectrum changes from $f_\nu \propto \nu$ to ν^{-1}. Therefore, somewhere in between these two frequencies the index would be 0.2. The Konus data for GRB 080319B found the spectral peak to be at 665 keV and the observations extended down to a minimum photon energy of 20 keV. Therefore, the IC spectral index of 0.2 at 20 keV requires $\nu_i/\nu_{\rm a} \sim 25$.

$$E_{\rm e} = \begin{cases} (3.4\times10^{49}\ {\rm erg})\ \eta_{1.4}^{-\frac{65}{21}} f_{{\rm op},1}^{-\frac{6}{7}} \nu_{{\rm ic}5.8}^{\frac{17}{7}} (\delta t)^{\frac{3}{7}} R_{16}^{\frac{23}{7}}, & R < R_{\rm tr}, \\ (3.3\times10^{50}\ {\rm erg})\ \eta_{1.4}^{-\frac{50}{24}} f_{{\rm op},1}^{-\frac{1}{4}} \nu_{{\rm ic}5.8}^{\frac{17}{8}} (\delta t)^{\frac{1}{8}} R_{16}^{\frac{19}{8}}, & R > R_{\rm tr}, \end{cases} \tag{45}$$

$$t_{\rm syn} = \begin{cases} (7.4\times10^{-4}\ {\rm s})\ \eta_{1.4}^{-5} f_{{\rm op},1}^{-3} \nu_{{\rm ic}5.8}^{3} (\delta t) R_{16}^{5}, & R < R_{\rm tr}, \\ (2\ {\rm s})\ \eta_{1.4}^{-\frac{35}{24}} f_{{\rm op},1}^{-\frac{7}{8}} \nu_{{\rm ic}5.8}^{\frac{31}{16}} (\delta t)^{\frac{1}{16}} R_{16}^{\frac{29}{16}}, & R > R_{\rm tr}, \end{cases} \tag{46}$$

$$t_{\rm ic} = \begin{cases} \frac{2.1\ {\rm s}}{L_{\rm obs,52}}\ \eta_{1.4}^{\frac{5}{7}} f_{{\rm op},1}^{\frac{3}{7}} \nu_{{\rm ic}5.8}^{-\frac{5}{7}} (\delta t)^{-\frac{5}{7}} R_{16}^{\frac{13}{7}}, & R < R_{\rm tr}, \\ \frac{0.7\ {\rm s}}{L{\rm obs,52}}\ \eta_{1.4}^{\frac{5}{24}} f_{{\rm op},1}^{\frac{1}{8}} \nu_{{\rm ic}5.8}^{-\frac{9}{16}} (\delta t)^{-\frac{9}{16}} R_{16}^{\frac{37}{16}}, & R > R_{\rm tr}, \end{cases} \tag{47}$$

$$f_{{\rm ic}-3} = \begin{cases} 7.1\times10^{-2}\ \eta_{1.4}^{-\frac{40}{21}} f_{{\rm op},1}^{\frac{6}{7}} \nu_{{\rm ic}5.8}^{\frac{11}{7}} (\delta t)^{\frac{4}{7}} R_{16}^{-\frac{2}{7}}, & R < R_{\rm tr}, \\ 7.8\times10^{-3}\ \eta_{1.4}^{-\frac{35}{12}} f_{{\rm op},1}^{\frac{1}{4}} \nu_{{\rm ic}5.8}^{\frac{15}{8}} (\delta t)^{\frac{7}{8}} R_{16}^{\frac{5}{8}}, & R > R_{\rm tr}. \end{cases} \tag{48}$$

Fig. 1 shows the dependencies of a number of quantities as functions of the only free parameter in the model: R_{16}. The lower solid line in the top-left panel shows the predicted gamma-ray flux $f_{{\rm ic}-3}$ (based on equation 48) and immediately indicates a major problem. If, as we suggested earlier, $R_{16} \sim R_{{\rm tr},16}$, then the peak IC flux $f_{\rm ic}$ that the model predicts falls short of the observed flux by nearly a factor of 100.

In Appendix A, we discuss possible sources of error in our estimate of the IC flux. We show that the uncertainty in $f_{\rm ic}$, even after allowing for inhomogeneities in the source, is no larger than a factor of order unity. The largest error is that we have overestimated $\nu_{\rm a}$ by a factor of $\sim$1.5 by not including the expansion of the source during the time it takes for a photon to cross the shell (see Appendix A). The effect of this is that $f_{\rm ic}$ is underestimated by a factor of $\sim$2.5 due to its dependence on $\nu_{\rm a}$ via η. Even after correcting for this (upper solid line in upper-left panel in Fig. 1), the theoretically calculated gamma-ray flux is still smaller than the observed value by a factor of $\sim$30. This discrepancy is

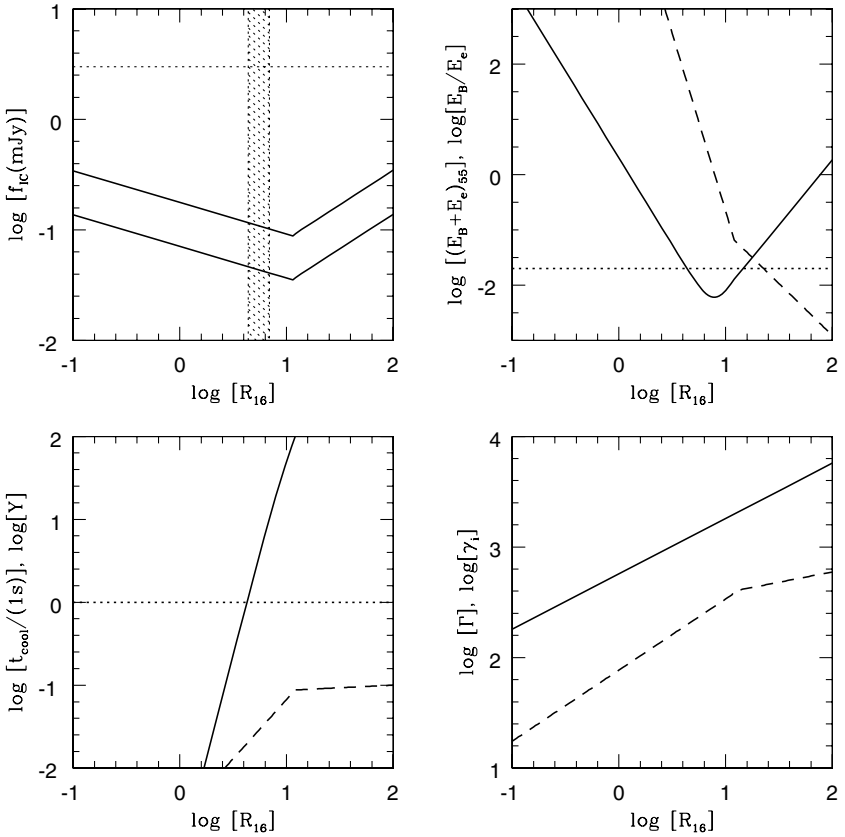

Figure 1. Top-left panel shows the IC flux in GRB 080319B at 650 keV predicted by the internal shock model. The lower line is from equation (48) and the upper line corresponds to a factor of 2.5 larger flux to allow for the expansion of the source during a photon crossing time, which was not included in the calculations presented in Sections 3 and 4 (see the Appendix for details and for a discussion of uncertainties in $f_{\rm ic}$ and $\nu_{\rm a}$). The shaded band is the region of the source radius R_{16} that is favoured by various constraints (see text for details). For these values of R_{16}, the predicted IC flux falls short of the observed gamma-ray flux (horizontal dotted line) by a factor of $\gtrsim$30. Top-right panel: the solid line shows the total isotropic energy in a single variability spike in the gamma-ray LC. The dotted line shows the maximum energy allowed. The dashed line shows $E_B/E_{\rm e}$. Bottom-left panel: the solid line shows the cooling time in units of the variability time (1 s); this should be $\gtrsim$1 since the low-energy spectral index was positive. The dashed line shows the Compton Y. Bottom-right panel: the solid line shows the bulk Lorentz factor Γ, and the dashed line shows the typical Lorentz factor of electrons γ_i.

much too large to be overcome by minor adjustments to the model. We thus conclude that the internal shock model with $R_{16} \sim R_{\rm tr,16}$ is ruled out for GRB 080319B.

One way to mitigate this problem is to select values of R_{16} that are either very much smaller or very much larger than $R_{\rm tr,16}$. However, as Fig. 1 shows, we need to modify R_{16} by a huge factor, which immediately leads to other problems.

The top-right panel indicates one of the problems we face. This panel shows the total isotropic energy of the source ($E_B + E_{\rm e}$) in units of 10^{55} erg. We see that shifting R_{16} substantially away from $R_{\rm tr,16}$ causes the total energy to become unphysically large. A reasonable upper limit to the total energy is 10^{55} erg,[8] which corresponds to an energy of $\sim 2 \times 10^{53}$ erg in each spike in the gamma-ray LC. The energy estimates in equations (44) and (45) refer to the energy per spike, and the limit on the total energy is shown by the dotted line in the top-right panel. We see that the energy constraint restricts R_{16} to lie within the range 4.4–14.6. Within this range of R_{16}, we have approximate equipartition between E_B and $E_{\rm e}$ (see the dashed line), which is desirable, whereas choosing other values of R_{16} would cause large deviations from equipartition.

The bottom-left panel in Fig. 1 shows another set of problems. Given the huge luminosity of GRB 080319B, we expect the source to be radiatively efficient, which means that $t_{\rm cool}$ must be comparable to the variability time $t_{\rm var} \sim \delta t \sim 1$ s. We see that the cooling time $t_{\rm cool}$, calculated according to

$$\frac{1}{t_{\rm cool}} = \frac{1}{t_{\rm syn}} + \frac{1}{t_{\rm ic}}, \tag{49}$$

is within a factor of 10 of the variability time only for models with R_{16} in the narrow range 2.7–6.9. (The variation of $t_{\rm cool}$ with R_{16} is extremely steep, so the condition $t_{\rm cool} \sim t_{\rm var}$ is very restrictive.) Combining this constraint with the one we obtained earlier from the total energy, the allowed range of R_{16} is limited to 4.4–6.9, shown as the hatched vertical band in the top-left panel in Fig. 1. We also see from the bottom-left panel that the Compton Y is less than 0.1 for most models, and extremely small, $Y \ll 0.1$, for small values of R_{16}. Since Y determines the fraction of the source luminosity that comes out in gamma-rays, and since GRB 080319B (indeed, any GRB) is a strong gamma-ray source, it seems unlikely that Y could be this small.

Finally, the bottom-right panel in Fig. 1 shows the dependence of the bulk Lorentz factor Γ and the random electron Lorentz factor γ_i on R_{16}. Models with $R_{16} \sim R_{\rm tr,16}$ predict reasonable values $\sim 10^2$–10^3 for both Lorentz factors, but models with very different values of R_{16} predict either unusually low or unusually high values.

In summary, all the indications suggest that the optical and gamma-ray radiation in GRB 080319B were produced at a radius $R \sim$ few $\times$ 10^{16}–10^{17} cm. But at this radius, the internal shock model predicts a negligibly small gamma-ray flux. We are thus forced to conclude that the internal shock model, at least in its standard form, is definitely ruled out for GRB 080319B.

4.1 Other versions of the internal shock model

We now consider whether we can get around the above difficulty by modifying the internal shock model. We begin by noting that as long as the gamma-ray emission is IC – something that is required by the low-energy spectrum $f_\nu \propto \nu^{0.5}$ at early times (Section 2) – and the seed synchrotron photons are produced in the same source region as the γ-ray photons, equation (48) is valid. This equation predicts an unacceptably low flux in the gamma-ray band. Therefore, if we wish to save the internal shock model, we must give up the assumption that all the radiation came from the same region of the source.

Let us assume that the seed photons for IC scattering are produced by the same source that gave us the optical flash. We will call this the *optical region* of the source. Let us assume that these seed photons are IC-scattered in a different region, the *gamma-ray region*. We now show that the electron Lorentz factors γ_i in the two regions are very similar.

Let us suppose that γ_i in the optical region differs from that in the gamma-ray region. Then, the self-IC radiation from the optical region will introduce a second IC component in the observed spectrum, with a peak at a different photon energy. Equation (48) is valid for any SSC process, so we can use it to estimate the flux in the second peak. If the IC peak from the optical region is at a higher photon energy than 650 keV by a factor of >2.5, then equation (48) shows that the flux in this component will be larger than the observed flux (note that $f_{\rm ic} \propto \nu_{\rm ic}^{11/7}$ as per equation 48, and the observed flux above 650 keV declined as $\nu^{-2.87}$). On the other hand, if the self-IC radiation peaks at an energy much less than 650 keV, the magnetic energy in the source will increase very rapidly ($E_B \propto \nu_{\rm ic}^{-26/7}$; equation 44). Since the energy is already close to the maximum limiting value we can accept, this option is also ruled out.

Therefore, the values of γ_i in the optical and gamma-ray regions must be nearly the same. This tight relation between the Lorentz factors in the two regions suggests that the optical and gamma-ray sources are very likely the same region. Even if they are not, the similarity of their parameters means that the large discrepancy in the gamma-ray flux discussed previously will survive unchanged.

A related idea is that there are two populations of electrons with different values of γ_i within the same source. One population is responsible for the seed photons and the other for the IC scattering. This possibility can be ruled out by the same argument.

This leads us to consider a model in which part of a shell is magnetized – this is where optical photons are produced – and the rest has a much weaker magnetic field (in order to avoid overproducing synchrotron flux) but contains about 30 times more electrons in order

[8] The isotropic energy release for GRB 080319B in the 20 keV–7 MeV band was 1.3×10^{54} erg. The radiative efficiency for GRBs varies widely from burst to burst but is generally larger than $\sim$10 per cent (Panaitescu & Kumar 2002). Therefore, the total energy release in GRB 080319B is expected to be $\lesssim 1.3 \times 10^{55}$ erg, and so we take $(E_B + E_{\rm e}) \lesssim 10^{55}$.

to produce the observed ∼3 mJy γ-ray flux via IC scattering. This situation can arise, for instance, when magnetic field decays downstream of a shock front, as suggested in Kumar & Panaitescu (2008). However, this proposal suffers from serious problems that these authors have pointed out in their paper. The solution requires magnetic field to decay on a length-scale that is about 5 per cent of the shell thickness or about 10^7 plasma skin depth . This scale corresponds to no particular physical scale in the system and is quite arbitrary. An even more severe problem is that the model cannot account for the shorter time-scale variability of gamma-rays compared to the optical; in fact, the natural expectation is the opposite in this model.

Note that Fig. 1 indicates an extremely narrow range of R for the radiating medium. It is hard to believe that a large number of independent shells ejected from the central source would all collide at exactly this radius. In addition, as we noted earlier, the radius R of the source is uncomfortably large for the internal shock model. Both of these features would be explained naturally if we assumed that the internal shocks are not between independent shells, but rather between successive shells and the outermost shell, which is decelerating after colliding with the external medium. This is a variation on the general idea of internal shocks (with a strong hint of the forward shock (FS) model, see Section 5.2.2), which at least provides an explanation for the radius of the source. However, this model can be ruled out for two reasons. As with all other variants, this model cannot explain the magnitude of the IC flux unless the magnetic field occupies a small fraction of the shocked shell, about 5 per cent of the ejecta width or 10^7 plasma skin depths. Furthermore, it predicts that the pulse width should increase with time, which is inconsistent with the observed data for GRB 080319B which show, if anything, that the last few pulses in the gamma-ray LC were somewhat narrower than the initial few pulses.

Having considered these and other ideas, we believe that it is impossible to explain the observations of GRB 080319B with any reasonable version of the internal shock model. Fortunately, there is an alternative model which invokes relativistic turbulence in the radiating fluid. We now apply this model to GRB 080319B.

5 RELATIVISTIC TURBULENCE MODEL FOR GRB 080319B

The basic kinematic features of the relativistic turbulence model are described in Narayan & Kumar (2009; see also Lazar, Nakar & Piran 2009).[9] In brief, this model explains the observed variability in GRB LCs by postulating an inhomogeneous relativistic velocity field in the GRB-producing medium (which we refer to as the 'shell' because of its shell-like morphology in the host galaxy frame). The beaming effect of the turbulent eddies causes large amplitude fluctuations in the observed flux. Despite being inhomogeneous, the model is radiatively efficient in the sense that the whole medium radiates and the observer receives a fair share of the radiated luminosity. This important feature, which is a direct consequence of beaming, allows the model to overcome the arguments of Sari & Piran (1997) against inhomogeneous GRB models. The reader is referred to Narayan & Kumar (2009) for details.

Since the relativistic turbulence model has a natural explanation for the observed variability, equation (4) relating the variability time-scale δt to R and Γ is no longer needed. Instead, the quantity $R/2\Gamma^2 c$ determines the *total* burst duration t_γ. We thus have

$$t_\gamma \sim \frac{R(1+z)}{2c\Gamma^2} = (1.7\times10^4\,\mathrm{s})R_{15}\Gamma^{-2}(1+z). \tag{50}$$

Since $t_\gamma \sim 50$ s for GRB 080319B, whereas $\delta t \sim t_{\rm var} \sim 1$ s, this modification has a rather profound effect on the results.

In the relativistic turbulent model, we consider turbulent eddies with a typical bulk Lorentz factor $\gamma_{\rm t}$ in the frame of the shell, and a typical size $\sim R/(\gamma_{\rm t}\,\Gamma)$ in the comoving frame of an eddy. The eddies are volume-filling, so there are $\sim\gamma_{\rm t}^3$ eddies in a causally connected region of volume $\sim R^3/\Gamma^3$. We assume that the velocity field of eddies changes direction by $\sim 2\pi$ on the light-crossing time-scale $\sim R/(c\gamma_{\rm t}\,\Gamma)$. In this case, the probability that an eddy, some time during its life, will move towards the observer with a velocity vector within an angle $(\gamma_{\rm t}\Gamma)^{-1}$ of the line of sight is $\sim\gamma_{\rm t}^{-1}$ (Narayan & Kumar 2009).[10] Therefore, over the course of the burst, a given observer will receive emission from $\sim\gamma_{\rm t}^2$ eddies, with each eddy producing a pulse of radiation lasting a time (see Narayan & Kumar 2009 for details).

$$t_{\rm var} \sim t_\gamma/\gamma_{\rm t}^2. \tag{51}$$

Since GRB 080319 has $t_{\rm var} \sim t_\gamma/100$, we infer that $\gamma_{\rm t} \sim 10$ for this burst. Note that, at any given time, the observer receives radiation from only one eddy on average.

We assume that the fluid in the shell consists of eddies and an inter-eddy medium. The latter is produced when eddies collide and shock. Let us take the thermal Lorentz factor of electrons within an eddy to be γ_{it}. The thermal Lorentz factor of electrons in the inter-eddy medium follows from energy conservation when eddies collide, and is $\sim\gamma_{it}\gamma_{\rm t} \equiv \gamma_i$. Similarly, if we take the magnetic field in the inter-eddy frame to be B, then the comoving magnetic field in an eddy is $B/\gamma_{\rm t}^{1/2}$, assuming that the magnetic energy is roughly conserved when eddies dissipate.

[9] The idea that variability could arise from relativistic motions of independent clumps in the source was originally proposed by Lyutikov & Blandford (2003). However, they merely stated the idea and did not describe a specific kinematic model or give any details. The papers by Narayan & Kumar (2009) and Lazar et al. (2009, see also Lyutikov 2006a) give the necessary details for modelling GRB observations.

[10] It is not essential that eddies experience smooth continuous acceleration as described here; in fact, given their supersonic speeds, this is unlikely. A more likely situation is that each eddy travels along $\sim\gamma_{\rm t}$-independent ballistic trajectories, each of order the mean free path $\sim R/(\gamma_{\rm t}\Gamma)$ in length (as measured in the shell frame), during the duration of the burst. This would give essentially the same results, as discussed in Narayan & Kumar (2009). In this sense, the relativistic turbulent model does not necessarily require 'turbulence' in the strict sense of the term, but merely requires random relativistic motions of independent clumps, as envisaged by Lyutikov & Blandford (2003).

Using these scalings we see that the peaks of the synchrotron spectrum (as measured in the shell frame) for inter-eddy and eddy emissions are proportional to $B\gamma_i^2$ and $B\gamma_i^2\gamma_t^{-3/2}$, respectively.

Let us take the average number of electrons in an eddy to be N_{ed}, and the total number of electrons in the inter-eddy medium in a volume $(R/\Gamma)^3$ (the volume of a causally connected region) to be N_i. For simplicity, let us assume that the total number of electrons in all the γ_t^3 eddies is of the order of N_i, i.e. half of the fluid in the shell is in eddies and the other half is in the inter-eddy medium. Thus we have $N_{ed} \sim N_i/\gamma_t^3$.

At any given time, only one eddy will produce beamed radiation towards the observer. The peak synchrotron flux from this eddy is proportional to $\sim BN_{ed}\gamma_t^{3/2}\Gamma^3 \sim BN_i\Gamma^3/\gamma_t^{3/2}$. Here we have made use of the fact that, at a fixed observer time, the observer receives radiation from only a fraction of the electrons in the eddy, $\sim N_e/\gamma_t$, due to the time dependence of eddy velocity direction. The peak synchrotron flux from the inter-eddy medium is $\sim BN_i\Gamma^3$, which is larger than the peak flux from the eddy by a factor of $\sim\gamma_t^{3/2}$. The synchrotron flux in a fixed observer band above the peak frequency is larger for the inter-eddy medium by an additional factor of $\gamma_t^{3(p-1)/4}$. We thus conclude that the synchrotron emission observed in the optical band is completely dominated by the inter-eddy medium. We therefore ignore eddies when we estimate the optical synchrotron flux.

The situation is different for the IC emission. Let us write the synchrotron flux as seen by a typical electron in the inter-eddy medium as f_{syn} (this is easily estimated from the calculation above). The observed IC luminosity due to electrons in the inter-eddy medium f_{ic}^{ie} is then

$$f_{ic}^{ie} \propto \sigma_T f_{syn} N_i \Gamma^3, \tag{52}$$

while the IC emission from an eddy pointing towards the observer f_{ic}^{eddy} is

$$f_{ic}^{eddy} \propto \sigma_T(\gamma_t f_{syn})N_{ed}(\Gamma\gamma_t)^3/\gamma_t \sim \sigma_T f_{syn} N_i \Gamma^3. \tag{53}$$

We see that the two contributions are equal. Therefore, both components in the shell fluid contribute equally to the gamma-ray IC flux. Of course, the inter-eddy contribution will vary smoothly over the duration of the burst, whereas the contribution from the eddies will be highly variable.

Using these results, we may easily estimate the values of various parameters in GRB 080319B corresponding to the relativistic turbulence model. Note that, since the synchrotron radiation, or optical flux, comes from the inter-eddy plasma, it satisfies the same equations as derived in Section 4. Moreover, the IC flux has no dependence on the Lorentz factor of turbulent eddies (equation 53). Therefore, equations (39)–(48) may be directly used for the relativistic turbulence model provided we replace δt with the burst duration 50 s, and take N_e, E_B, E_e and f_{ic} to be two times larger than the values given by these equations (the factor of 2 is to count both the eddies and the inter-eddy medium).

Setting $\delta t = 50$ s (equation 50), $f_{op} = 10$ Jy, $\nu_{ic} = 650$ keV and $\eta_{1.4} = 1$ (i.e. $\eta = \nu_i/\nu_a \approx 25$) into equation (39), we obtain the transition radius

$$R_{tr} = 2 \times 10^{16}\,\mathrm{cm}. \tag{54}$$

The other parameters follow from equations (40)–(48):

$$\Gamma = 81 R_{16}^{1/2}, \tag{55}$$

$$\gamma_i = \begin{cases} 254\, R_{16}^{\frac{9}{14}}, & R < R_{tr}, \\ 349\, R_{16}^{\frac{3}{16}}, & R > R_{tr}, \end{cases} \tag{56}$$

$$N_e = \begin{cases} 9.4 \times 10^{52}\ R_{16}^{\frac{15}{7}}, & R < R_{tr}, \\ 1.3 \times 10^{53}\ R_{16}^{\frac{27}{16}}, & R > R_{tr}, \end{cases} \tag{57}$$

$$Y = \begin{cases} 2.1 R_{16}^{\frac{10}{7}}, & R < R_{tr}, \\ 5.5\, R_{16}^{\frac{1}{16}}, & R > R_{tr}, \end{cases} \tag{58}$$

$$E_B = \begin{cases} (2.6 \times 10^{53}\,\mathrm{erg})\ R_{16}^{-\frac{22}{7}}, & R < R_{tr}, \\ (1.9 \times 10^{52}\,\mathrm{erg})\ R_{16}^{\frac{1}{2}}, & R > R_{tr}, \end{cases} \tag{59}$$

$$E_e = \begin{cases} (1.3 \times 10^{51}\,\mathrm{erg})\ R_{16}^{\frac{23}{7}}, & R < R_{tr}, \\ (2.6 \times 10^{51}\,\mathrm{erg})\ R_{16}^{\frac{19}{8}}, & R > R_{tr}, \end{cases} \tag{60}$$

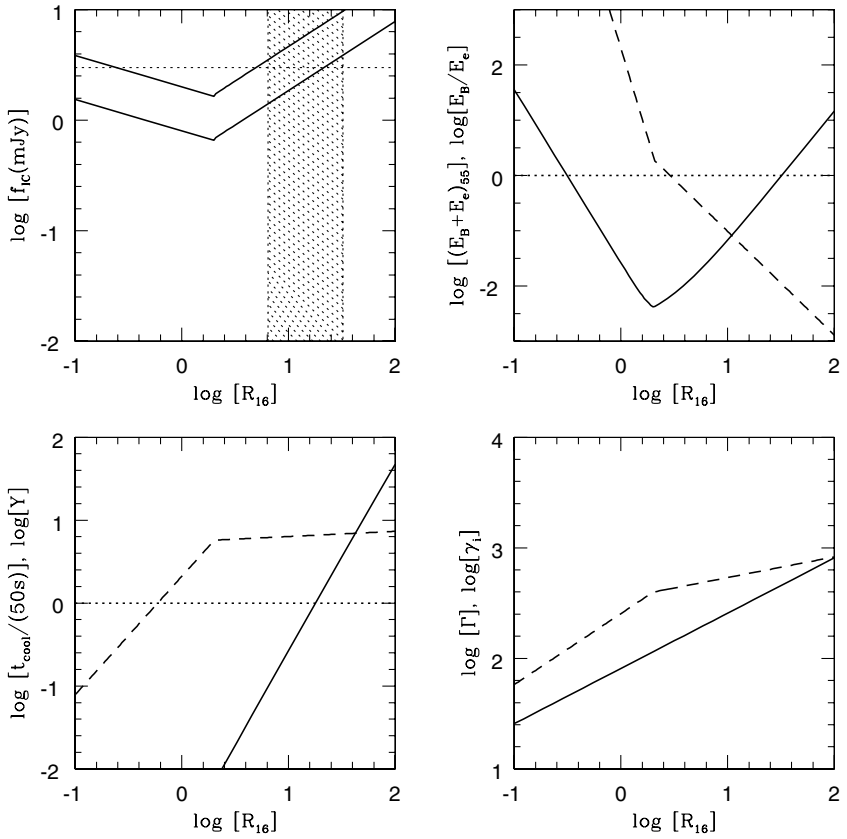

Figure 2. Similar to Fig. 1, but for the relativistic turbulence model. Top left: predicted (solid lines) and observed (dotted line) $f_{\rm IC}$. Top right: $E_{\rm B55} + E_{\rm e55}$ (solid line) and $E_{\rm B}/E_{\rm e}$ (dashed line). Bottom left: $t_{\rm cool}$ (solid line) and Y (dashed line). Bottom right: Γ (solid line) and γ (dashed line). Note that the predicted IC flux (solid lines in the top-left panel) is perfectly consistent with observations (horizontal dotted line). The shaded region indicates the range of source radii R_{16} that is consistent with constraints on the total energy (solid line in the top-right panel) and the cooling time (solid line in the bottom-left panel) constraints (see text for details). We note that the ratio of IC and synchrotron luminosities is larger by ∼5 than the value of Y shown as a dashed line in the lower-left panel (see equation 9 for the definition of Y) due to two different effects: (1) the commonly used Compton Y is larger than Y in equation (9) by a factor of 2 due to p-dependent factors and (2) the synchrotron photon energy density inside the shell is larger than the naive estimate of $L_{\rm syn}/(4\pi R^2 c)$ by a factor of ∼3.

$$t_{\rm syn} = \begin{cases} (0.3\,{\rm s})\ R_{16}^{5}, & R < R_{\rm tr}, \\ (2.8\,{\rm s})\ R_{16}^{\frac{29}{16}}, & R > R_{\rm tr}, \end{cases} \tag{61}$$

$$t_{\rm ic} = \begin{cases} \frac{0.1\,{\rm s}}{L_{\rm obs,52}}\ R_{16}^{\frac{13}{7}}, & R < R_{\rm tr}, \\ \frac{0.07\,{\rm s}}{L_{\rm obs,52}}\ R_{16}^{\frac{37}{16}}, & R > R_{\rm tr}, \end{cases} \tag{62}$$

$$f_{\rm ic-3} = \begin{cases} 0.80 R_{16}^{-\frac{2}{7}}, & R < R_{\rm tr}, \\ 0.44 R_{16}^{\frac{5}{8}}, & R > R_{\rm tr}. \end{cases} \tag{63}$$

As discussed above, we include only the inter-eddy medium for calculating the synchrotron component of the emission, but we include both the eddies and the inter-eddy medium when calculating the IC component. The synchrotron cooling time given by equation (61) applies only to electrons in the inter-eddy medium; the time-scale is larger by a factor of $\gamma_{\rm t}$ for electrons in eddies. We note that the IC flux should be increased by a factor of 2.5 to allow for the expansion of the source shell (Appendix A). Also, the flux will be larger by a factor of $N_{\rm ed}\gamma_{\rm t}^3/N_i$ than given in equation (63) if there are more electrons in eddies than in the inter-eddy medium.

5.1 Relativistic turbulence: a consistent model for GRB 080319B

Fig. 2 is similar to Fig. 1, but shows what happens when we use the relativistic turbulent model. We find a very good match both with the observations and with various consistency conditions when we choose $R \approx 10^{17}$ cm. For this choice of R, we have (i) gamma-ray flux $f_{\rm ic-3}$ predicted to be close to the observed flux, (ii) modest requirement for the total isotropic energy $\sim 10^{54}$ erg, (iii) $E_B \sim E_{\rm e}/10$, i.e. approximate equipartition between magnetic and thermal energy, (iv) $t_{\rm cool} \sim 50$ s, i.e. the cooling time is comparable to the burst duration and thus

consistent with efficient radiation, (v) $Y\sim$ few,[11] i.e. consistent with gamma-rays dominating the emission, (vi) $\Gamma \sim 250$ as inferred for GRBs, in general, from a variety of observations (Lithwick & Sari 2001) and (vii) electron Lorentz factor in the inter-eddy medium $\gamma_i \sim 500$ and in eddies $\gamma_i/\gamma_t \sim 50$, which are quite reasonable.

We note that the ratio of luminosity in the second IC component to the first IC component is of the order of unity even though the ratio of total luminosity in the first IC and synchrotron components is about 20. The reason is that for the best-fitting model the bulk Lorentz factor of the source is 250 whereas the electron Lorentz factor is 540. Therefore, since the peak of the first IC spectrum in the source comoving frame is at 5.2 keV, the second IC scattering lies in the Klein–Nishina regime, which reduces the effective second Compton Y (compared with the first Y) by a factor of $\sim$5. Moreover, the average electron Lorentz factor decreases with time for a relativistically expanding source, after the heating episode is turned off, and this accounts for an additional factor of $\sim$3 decrease in the luminosity of the second Compton component.

The shaded band in Fig. 2 shows the range of R_{16} that is consistent with our two primary constraints. First, we require the total isotropic energy over the duration of the burst to be no larger than 10^{55} erg. This constrains R_{16} to lie in the range 0.31–32. Secondly, we require the cooling time $t_{\rm cool}$ to lie within a factor of 10 of the burst duration 50 s. This gives the constraint $6.5 < R_{16} < 50$. Requiring both conditions to be satisfied simultaneously restricts R_{16} to lie in the range 6.5–32, as shown in Fig. 2. Within this range, the predicted gamma-ray flux agrees remarkably well with observations.

Note that the deceleration radius for the blast wave is

$$R_{\rm d} = \left(\frac{3E\delta t}{4\pi\bar{n}m_{\rm p}c(1+z)}\right)^{1/4} = 1.1\times10^{17}\,{\rm cm}\ E_{54}^{1/4}(\delta t/50s)^{1/4}\bar{n}^{-1/4}, \quad (64)$$

where $\bar{n}$ is the mean particle density of the circumstellar medium within the radius $R_{\rm d}$. It is interesting that $R_{\rm d}$ lies in the middle of the allowed range for the source distance R. It provides independent confirmation that the prompt radiation in GRB 080319B was not produced in internal shocks – there is no reason why internal shocks should occur at the deceleration radius.

In addition to the various successes described above, the relativistic turbulence model explains all the major qualitative features observed in the γ-ray and optical LCs of GRB 080319B during the initial $\sim10^2$ s, i.e. before the onset of FS emission.

Since the gamma-ray emission (via IC) arises partly from eddy electrons and partly from the inter-eddy medium, we expect the gamma-ray LC to consist of a smooth slowly varying component plus a large number of sharp spikes. This is the case for most GRBs, including GRB 080319B (e.g. fig. 1 in Racusin et al. 2008). The relative fluxes in the two components provide information on the relative numbers of electrons in the two media. We assumed in our model (for convenience) that the numbers are roughly equal and this is reasonably consistent with the observations. As already mentioned, by combining the γ-ray variability time of $\sim$0.5 s with the burst duration of 50s, we infer that $\gamma_t \sim 10$ for GRB 080319B.

Since the synchrotron emission is generated by inter-eddy electrons, the optical LC is expected to be much less variable than the IC-dominated gamma-ray emission. This is indeed the case for GRB 080319B. At the same time, the overall duration of the optical and gamma-ray LCs are expected to be similar, as observed.

The optical LC of GRB 080319B showed an initial rapid rise by more than an order of magnitude in flux (fig. 3 in Racusin et al. 2008), whereas the γ-ray LC showed a much less rapid rise. This finds a natural explanation. According to the turbulent model of GRB 080319B, the synchrotron frequency ν_i was below the optical band. Therefore, the optical spectrum is predicted to be very soft: $F_\nu \propto \nu^{-2.8}$. If we assume that ν_i initially started off at a somewhat lower frequency and later settled down at a larger value, say by a factor of $\sim$3, then the optical flux would increase by nearly a factor of 20. This explanation might indicate that the gamma-ray peak energy $\nu_{\rm ic}$ should also increase with time, whereas in fact $\nu_{\rm ic}$ decreased by a small amount (from 750 to 550 keV). To explain this, we would need to invoke that the electron Lorentz factor γ_i decreased by a factor of about 2 during this time. Note that the reason for the much less rapid increase of the γ-ray flux is that the synchrotron peak flux, which is proportional to the number of electrons and the magnetic field strength, is a slowly varying function of time.

Another property of the relativistic turbulence model is that we should continue to see emission in the γ-ray band for a time duration somewhat longer than the prompt optical LC duration. The reason is that there is a very high probability that a few eddies lying a little bit outside of Γ^{-1} will point towards the observer, thereby slightly lengthening the burst duration in the gamma-ray band (see fig. 1 in Narayan & Kumar 2009). This effect is clearly seen in the LCs of GRB 080319B; the optical LC started falling off at 43 s whereas the steep decline of the gamma-ray LC began at 51 s.

A prediction of the model is that the synchrotron and IC spectra should be the same. In particular, since our solution for GRB 080319B requires $R \sim 10^{17}$ cm $> R_{\rm tr}$, or $\nu_i < 2$ eV, the spectral index in the optical band during the burst should have been the same as the high-energy index in the gamma-ray band, i.e. $\beta = 2.87$. It is unfortunate that there were no measurements of optical spectrum during the burst. The first measurement was at $t \sim 10^2$ s when it was found that $\beta = 0.55$ or $f_\nu \propto \nu^{-0.55}$ (Wozniak et al. 2008). This measurement would seem to call into question the prediction of the SSC model.

[11] The ratio of energies in the IC radiation and the synchrotron emission is $\sim 5Y$. This is in part because the parameter Y, defined in equation 9, differs from the commonly used Compton Y parameter by a factor of $\sim$2 (due to p-dependent factors not included in equation 9), and in part because the mean synchrotron photon energy density in the shell is larger than $L_{\rm syn}/(4\pi R^2 c)$ by a factor of 3. The ratio of the observed fluence in gamma-ray and optical bands is $\sim$80, which is larger than $5Y$ by a factor of $\sim$2.5. This last factor arises naturally in the model since the optical band lies above the peak of the synchrotron spectrum. Therefore, the synchrotron peak flux $f_{\rm syn}$ is larger than the observed optical flux $f_{\rm op}$.

It is, however, interesting to note that the optical LC showed a sharp break at about 90 s. Prior to this time, the flux scaled as $t^{-5.5}$ and after this time the flux decreased as $t^{-2.8}$ [see fig. 2 of Kumar & Panaitescu (2008) or Racusin et al. (2008)]. This suggests that 90 s marked a transition from one source of radiation to another, and that $\beta = 0.55$ at $\sim 10^2$s corresponds to the second source which gave rise to the $f_\nu \propto t^{-2.8}$ part of the LC and was possibly unrelated to the prompt radiation.

The optical LC decline of $t^{-5.5}$ between 43 and 90 s is roughly consistent with the expectation of the relativistic turbulence model after the source is turned off at $t \sim 43$ s; the observed radiation in this case is the large-angle emission (LAE) from photons arriving from angles larger than Γ^{-1}, leading to a flux decline of $t^{-2-\beta}$ or $\sim t^{-5}$ when $\beta \sim 3$ (Kumar & Panaitescu 2000b). So the steeply declining optical LC at the end of the GRB provides an indirect confirmation of a steep spectrum in the optical band.

The gamma-ray LC in the 15–150 keV band at the end of the burst was seen to fall off even faster than the optical flux at the end of the burst. This is a puzzling behaviour, and unlikely to be due to LAE. The reason is that the spectral index in this band was close to zero during the burst, and therefore the LAE flux decline should be $\sim t^{-2}$ – unless the peak frequency fell off from 650 keV to less than 100 keV at the end of the burst which seems unlikely. The only natural explanation for the very steep decline of the γ-ray flux is that the velocity distribution of the relativistic eddies was anisotropic, with eddies preferentially pointing transverse to the local radius vector of the shell (possibly along the local magnetic field). In this case, the gamma-ray flux at the end of the burst would fall off much faster than the LAE flux because there would be very few eddies pointing towards the observer; in the extreme case where the velocity distribution is confined to the transverse plane, the gamma-ray flux would fall off on the time-scale of an individual pulse in the LC, i.e. $\sim$0.5 s.

What about the fall-off of the optical flux as $t^{-2.8}$ for $t \gtrsim 10^2$ s? It cannot be LAE for the reasons described above. We offer an explanation for this part of the optical LC that requires the GRB jet to be a Poynting outflow (see Section 5.2.4). A Poynting jet travelling outwards from the centre of the star cannot avoid sweeping up and accumulating some amount of baryonic material at its head. In subsequent jet expansion, this baryonic gas is cooled, and at the deceleration radius it is heated once again by the reverse shock (RS). The optical emission from this RS-heated gas might be responsible for the LC for $10^2 \lesssim t \lesssim 10^3$ s. We know from equation (68) below that $N_{\rm e}/N_{\rm RS} \sim 10$ (assuming that the kinetic energy in the baryonic head of the Poynting jet is of the order of the explosion energy). Therefore, the optical flux from the RS is a factor of $\sim$10 smaller than the prompt gamma-ray source. The more slowly declining RS flux took over from the very rapidly declining flux from the early GRB tail at $t \sim 10^2$ s, and continued to dominate the LC until the even more slowly declining, but weaker, FS optical emission took over at $t \sim 10^3$ s.

We note that the effect of a narrow jet, with opening angle $\sim\Gamma^{-1}$, is very weak on the emergent afterglow LC decay for a long period of time when the jet is propagating in a medium with density falling off as r^{-2} (Kumar & Panaitescu 2000a); the density in the circumstellar medium of GRB 080319B is in fact inferred to be r^{-2} by the late-time afterglow data (cf. Kumar & Panaitescu 2008; Racusin et al. 2008).

5.2 Where exactly is the turbulent region located?

As we have seen, the relativistic turbulence model gives robust estimates for various source parameters such as the radius, bulk Lorentz factor and energy of the shell, the number and typical Lorentz factors of the radiating electrons, etc. Using these results we now attempt to infer where the radiating region is located within the context of a dynamical model of GRBs.

5.2.1 Not in internal shocks

The internal shock model, including all reasonable variations, is firmly ruled out, as we have discussed in Section 4. Inclusion of relativistic turbulence within the context of this model will not salvage the situation unless we take δt to be the burst duration (as shown in Section 5). However, in that case we are dealing with a situation in which the emission region is close to the deceleration radius, which is no longer an internal shock.

The primary motivation for the internal shock model is to explain the rapid variability observed in the gamma-ray LCs of GRBs (Sari & Piran 1997). The relativistic turbulence model described in Narayan & Kumar (2009) has a completely different explanation for the variability. In particular, this model no longer needs to assume equation (4), which is the key relation in the internal shock model. Therefore, we see no reason to retain the internal shock picture.

5.2.2 Not in the forward shock

In the standard model of GRBs, the collision of the relativistic ejecta with the external medium causes a pair of shocks to be generated: a FS which is driven into the external medium and a RS which is driven into the ejecta.

We can rule out the FS by considering the number of electrons we need for producing the observed radiation. From equation (57) we see that the radiating region must have about 6×10^{54} electrons. However, the number $N_{\rm FS}$ of electrons/protons processed in the FS must satisfy, by a simple energy argument,

$$N_{\rm FS}\Gamma^2 m_{\rm p}c^2 = E/2, \quad \text{or} \quad N_{\rm FS} = \frac{2E(\delta t)}{m_{\rm p}c(1+z)R} = 2\times 10^{52} E_{54}(\delta t)_1 (1+z)^{-1} R_{16}^{-1}. \tag{65}$$

For the particular case of GRB 080319B, this gives $N_{\rm FS} \sim 10^{52}$, which is smaller than the number of electrons needed by a factor of $\sim 10^2$. This is a large discrepancy, so we can discard the FS as the location of the relativistic turbulence.

5.2.3 Relativistic turbulence in the reverse shock?

Could the relativistic turbulence be located in the RS? Let the GRB ejecta be composed of protons and electrons, and let us take the Lorentz factor of the RS front with respect to the unshocked ejecta to be $\Gamma_{\rm RS}$. By applying pressure equilibrium across the contact discontinuity between the FS and RS fluid, we find the number of electrons $N_{\rm RS}$ that have been processed through the RS to be

$$N_{\rm RS} = N_{\rm FS}\frac{\Gamma}{\Gamma_{\rm RS}}. \tag{66}$$

Using equations (55) and (65), and the parameters for GRB 080319B, we find

$$N_{\rm RS} = 1.3\times 10^{54}E_{55}R_{17}^{1/2}\Gamma_{\rm RS,1}^{-1}. \tag{67}$$

Thus, the ratio of the number of electrons needed for optical/gamma-ray radiation (equation 57) and $N_{\rm RS}$ is given by

$$\frac{N_{\rm e}}{N_{\rm RS}} = 5E_{55}^{-1}\Gamma_{\rm RS,1}^{-1}R_{17}^{19/16}. \tag{68}$$

If gamma-rays were to arise in the RS then we expect $E_{55}\sim 0.4$. The reason is that half the energy of the blast wave is in the RS at the deceleration radius, and this energy is efficiently radiated when the cooling frequency is close to ν_i, as seems to be the case for GRB 080319B. Moreover, we presumably require $\Gamma_{\rm RS}\gtrsim 10$ in order for the shocked gas to have a turbulent $\gamma_{\rm t}\sim 10$. The requirement that $t_{\rm cool}\sim 50$ s means that $R_{17}\sim 1$. Therefore, we find from the above equation that $N_{\rm e}/N_{\rm RS}\sim 10$. This ratio might be closer to unity provided that protons carry a much larger fraction of the blast wave energy, so that E_{55} is $\sim$1−2 rather than 0.4.

The interesting result that it is possible to have $N_{\rm e}\sim N_{\rm RS}$ suggests that the turbulence is perhaps produced in the RS-heated GRB ejecta. The ratio of energies in magnetic fields and particle kinetic energy in this case is $\sim$0.1 (Fig. 2), which is similar to the value derived for the Crab pulsar at the wind termination shock (Kennel & Coroniti 1984). Presumably, the turbulence is a natural consequence of a relativistic shock. For instance, the contact discontinuity surface separating the FS and RS regions is known to suffer from the Rayleigh–Taylor instability. Could this explain the turbulence? In the shell comoving frame, the growth rate of the Rayleigh–Taylor instability at the interface of a relativistic RS and FS can be shown to be

$$\omega^2 = fkg, \tag{69}$$

where $g\sim c^2\Gamma/R$ is the effective gravitational acceleration in the shell comoving frame, $k=2\pi\ell\Gamma/R$ is the wavenumber of the perturbation, $f=3/(8\Gamma_{\rm RS}^2-5)$ and $\Gamma_{\rm RS}$ is the Lorentz factor of the RS front with respect to the unshocked ejecta. For $\Gamma_{\rm RS}\gg 1$, the above equation reduces to

$$\omega\sim\frac{c\Gamma\ell^{1/2}}{\Gamma_{\rm RS}R}\sim\frac{\ell^{1/2}}{\Gamma_{\rm RS}\delta t'}, \tag{70}$$

where $\delta t'$ is the GRB duration in the shell comoving frame. Thus, the number of e-folds by which the Rayleigh–Taylor mode can grow is $\sim\omega\,(\delta t')\sim\ell^{1/2}\Gamma_{\rm RS}^{-1}$. The eddy scale ℓ of interest to the IC problem is $R/(\Gamma\Gamma_{\rm RS})$ or $\ell\sim\Gamma_{\rm RS}$. Perturbations on this scale will undergo $\Gamma_{\rm RS}^{-1/2}$ e-folds of growth, i.e. the amplitude increases by less than a factor of 2. Therefore, the Rayleigh–Taylor instability is not sufficiently potent to generate the highly relativistic turbulence we need.

Recently, Goodman & MacFadyen (2007) and Milosavljevic, Nakar & Zhang (2007) have discovered interesting instabilities, resulting from a clumpy circumstellar medium and an initially anisotropic blast wave, respectively, which lead to vorticity generation downstream of the shock front. These instabilities have been further studied by Sironi & Goodman (2007) and Milosavljevic et al. (2007) to investigate the generation of magnetic fields in relativistic shocks. Couch, Milosavljevic & Nakar (2008) have found another instability that generates vorticity downstream of a shock front even when the circumstellar medium is homogeneous and the blast wave isotropic. We have estimated the growth rate of these instabilities and find that these too fail to give rise to relativistic turbulence.

Of course, we cannot rule out the possibility that there might be other as yet unknown instabilities that might give rise to relativistic turbulence. Therefore, we are unable to discard the possibility that the prompt GRB emission originates in the RS.

5.2.4 Relativistic turbulence in the Poynting-dominated jet

A Poynting-dominated jet would have a weak RS (Kennel & Coroniti 1984; Zhang & Kobayashi 2005) and would not be consistent with the proposal considered in the previous section. On the other hand, such a jet probably undergoes various plasma instabilities at the deceleration radius. These instabilities would stir up the fluid into a state consistent with our model of relativistic turbulence. The instabilities would presumably heat up the electrons until quasi-equipartition is achieved, consistent with the results shown in Fig. 2.

According to equations (59) and (60), in our model $E_B/E_{\rm e}\sim 0.1$ at $R\sim 10^{17}$ cm. However, this does not rule out the Poynting outflow model. The reason is that in all of our formulae B really stands for the projection of the magnetic field vector perpendicular to the electron momentum vector, i.e. $B\sin\alpha$ where α is the pitch angle between the electron momentum and the magnetic field direction. For a random distribution of particle pitch angle, the difference between B and $B\sin\alpha$ is of the order of unity. However, when electrons have a non-zero average momentum along the local magnetic field, as might be the case for particles accelerated in reconnection regions, the difference can be large. For instance, when the average α is 0.3 the energy in magnetic fields is larger than that in equation (59) by a factor of $\sim$10, making the model consistent with equipartition.

Lyutikov & Blandford (2003) have suggested that the dissipation of magnetic energy in a Poynting-flux-dominated jet should occur at a distance of $\sim 3 \times 10^{16}$ cm due to current-driven instabilities (see Lyutikov 2006b for a concise summary of the model and for a comparison with the baryonic outflow model). Acceleration of electrons (and positrons) and plasma bulk flow along the magnetic field lines at roughly the local Alfvén speed are expected in the process of magnetic field decay/reconnection. These expectations of the Poynting outflow model are roughly consistent with our findings for GRB 080319B: emission generated at $R \approx 10^{17}$ cm and turbulent velocity field with Lorentz factor $\gamma_{\rm t} \sim 10$. However, the reason for a very soft particle spectrum, $p \sim 5$, is unclear (at least to us); numerical simulations of particle acceleration in reconnection regions generally find a hard particle spectrum (e.g. Larrabee, Lovelace & Romanova 2003).

Moreover, it is also not clear how $\gamma_{\rm t}$ and γ_i should be related to the bulk Γ of the pre-instability jet. Nor is it clear why the typical Lorentz factor of electrons should be a modest value $\gamma_i \approx 500$ with the kind of powerful accelerator one might expect in magnetic reconnections (other than the fact that it is energetically impossible to accelerate a large number of electrons, of the order of 10^{55}, to an average Lorentz factor much larger than $\sim$500). Further investigation is required to address these questions.

6 SUMMARY

We have shown in this paper that the gamma-ray and optical data for GRB 080319B rule out the popular internal shock model for generation of the prompt radiation. Zou et al. (2009) have independently reached a similar conclusion. According to the internal shock model, the duration ($\lesssim$1 s) of spikes in the gamma-ray LC sets an upper bound on the quantity $R/(2c\Gamma^2)$, where R is the radius of the source relative to the centre of the explosion and Γ is the bulk Lorentz factor. When we apply this condition, we find that it is impossible to fit the observed optical and gamma-ray flux simultaneously. Specifically, any model that fits the optical flux underpredicts the gamma-ray flux by nearly two orders of magnitude (Fig. 1). This is an unacceptably large discrepancy which cannot be eliminated with any reasonable modification of the internal shock model.

An equally powerful qualitative argument against the internal shock model is the fact that we find the radius R of the source to be constrained quite tightly by the observations. The energy required in magnetic field increases very rapidly as we decrease R, $E_B \propto R^{-22/7}$, whereas the energy in particles increases rapidly with increasing R, $E_{\rm e} \propto R^{17/7}$. Also, the cooling time of electrons becomes too short to be compatible with observations if $R < 3 \times 10^{16}$ cm.[12] In the internal shock model, all of these factors together very strongly constrain the location where the prompt emission in GRB 080319B was produced: $4 \times 10^{16} \lesssim R \lesssim 8 \times 10^{16}$ cm (see Fig. 1). This is problematic. According to the internal shock model, there is a large number of internal shocks among independent ejecta, with a separate shock producing each of the $\sim$50 spikes in the gamma-ray LC of GRB 080319B. Why would all the ejecta collide within such a narrow range of radius? Moreover, why should the radius be so close to the deceleration radius $R_{\rm d} \sim 10^{17}$ cm, where the ejecta meet the external medium and begin to slow down? This coincidence is suspicious.

The above problems are eliminated if we give up the internal shock model and consider instead a model in which the variability in the gamma-ray LC is produced by relativistic turbulence in the source with random eddy Lorentz factors $\gamma_{\rm t} \sim 10$. In this model, the quantity $R/(2c\Gamma^2)$ is no longer constrained to be less than 1 s, but only needs to be comparable to the burst duration $\sim$50 s (Lazar et al. 2009; Narayan & Kumar 2009). With this modification, we find that we obtain a remarkably consistent model of GRB 080318B (see Fig. 2) in which the prompt optical emission was produced by synchrotron emission and the gamma-rays were the result of IC scattering. The predicted gamma-ray flux is perfectly compatible with observations. Also, estimates of various quantities, such as the total energy, cooling time, Lorentz factor, etc., are all very reasonable and consistent (Section 5.1). The radius of the source is calculated to be in the range $6 \times 10^{16} < R < 3 \times 10^{17}$ cm; if we select a nominal value $R \sim 10^{17}$ cm, we obtain an excellent fit to all the observations without requiring an unphysically large amount of energy. (According to the model, the ratio of energies in the second IC component, which peaks at $\sim$30 GeV, and the first IC component is of the order of unity, so there is not likely to be a huge amount of radiation in an unobserved Gev–TeV region of the spectrum.)

In the context of a physical model, the picture that emerges is that the energy of the relativistic jet in GRB 080319B was converted to optical and γ-ray radiation either via a relativistic reverse shock when ejecta (composed of $\rm p^+$s and $\rm e^-$s) ran into the circumstellar medium or that much of the jet energy was in magnetic field that was dissipated, e.g. via reconnection events, close to the deceleration radius. Theoretically, it is difficult to understand how a RS might produce relativistic turbulence with $\gamma_{\rm t} \sim 10$ (Section 5.2.3). Also, it is easier to understand the optical data for the time period $10^2 \lesssim t \lesssim 10^3$ s if we assume a Poynting jet (Section 5.2.4). For these reasons we have a mild preference for the Poynting-dominated jet model.

A potential problem for the Poynting jet model is that the ratio of magnetic-to-particle kinetic energy is about 0.1 for our best solution (Fig. 2). However, this ratio is similar to that inferred for the pulsar wind termination shock for the Crab pulsar (Kennel & Coroniti 1984). Moreover, this ratio of 0.1 does not rule out the Poynting model for another reason which is that, in all of our formulae, B is the projection of the magnetic field perpendicular to the electron momentum vector. Thus, if electron momenta are preferentially parallel to the magnetic field, then the true E_B would be larger than our estimate (easily by a factor of 10 compared to the value given in equation 59), and we can have

[12] Collisions at a smaller radius would produce a weak optical flash with flux decreasing roughly as $\rm R^{11/12}$. The electrons would undergo very rapid cooling and produce a low-energy spectrum in the gamma-ray band of $f_\nu \propto \nu^{-1/2}$. Prompt optical observations of GRB 080319B show variations in the optical flux by less than a factor of 2 for much of the 50 s duration of the burst except at the beginning and the end. Moreover, the low-energy spectral index for the gamma-ray emission was greater than zero throughout the burst.

$E_B/E_e \sim 1$. Note that electrons are accelerated parallel to the magnetic field in reconnection regions and so this possibility is not as arbitrary as it might appear.

In the relativistic turbulence model, fluctuations in the observed gamma-ray LC are produced as a result of random relativistic variations in the velocity field of the source, with a turbulent Lorentz factor $\gamma_t \sim 10$. The model predicts that there should be $\sim\gamma_t^2 \sim 100$ spikes in the gamma-ray LC (Narayan & Kumar 2009), which is consistent with the ∼50 spikes seen in GRB 080319B. The optical synchrotron flux is dominated by the inter-eddy medium rather than eddies. Therefore, we expect much less variability in the optical flux, as was indeed observed.

The model can explain the sharp rise in the optical flux of GRB 080319B at the beginning of the burst. For this, we must postulate that the synchrotron peak frequency increased from ∼0.5 to ∼1.5 eV during the first ∼15 s. Since the synchrotron peak frequency ν_i was below the optical band (2 eV), the optical flux was smaller than the peak synchrotron flux by a factor of $(4/\nu_i)^{2.8}$ (the spectral index above the peak is known from gamma-ray observations). A modest increase in ν_i by a factor of 3 early in the burst would thus produce a factor of 20 increase in the observed optical flux. The reason that the gamma-ray flux increased by a much smaller factor during the same time is that the peak IC flux is proportional to $\tau_e N_e B$, which would change little during this time period.

The end of the gamma-ray prompt emission phase occurred ∼ 8 s after the prompt optical in GRB 080319B. This is probably a result of IC emission from turbulent eddies lying a bit outside of the primary $1/\Gamma$ cone, but which happened to point towards us because of a fortuitous alignment of their turbulent velocity (the probability for this happening is of the order of unity). Since much of the synchrotron emission comes from non-turbulent fluid in between eddies, the optical flux would not have a similar effect.

Before concluding, we note that the results presented here apply specifically to GRB 080319B. This was an exceptional burst – it was extremely bright in the optical, and had an unusually soft gamma-ray spectrum at energies above the peak. If these unusual features resulted because this burst had different dynamics and radiation physics than other GRBs, then our conclusions cannot be generalized to other bursts. However, we believe there is a reasonable likelihood that the peculiarities of GRB 080319B are due to peripheral issues – perhaps some parameters had extreme values – and that the underlying physics in this burst, the dynamics and radiation processes, are representative of all bursts. If this is the case, then our study indicates that we may need to shift from the internal shock paradigm to a different paradigm, e.g. the relativistic turbulent model described in this paper, to understand the prompt emission in GRBs.

ACKNOWLEDGMENTS

PK is grateful to Rodolfo Barniol Duran for checking all equations in this paper, and Milos Milosavljevic for a number of useful discussions regarding relativistic turbulence. We thank the referee for insightful comments.

REFERENCES

Barniol Duran R., Kumar P., 2008, MNRAS, in press (arXiv:0806.1226)
Couch S. M., Milosavljevic M., Nakar E., 2008, ApJ, 688, 462
Cucchiara A., Fox D., 2008, GCN 7456
Dermer C. D., Chiang J., Botcher M., 1999, ApJ, 513, 656
Golenetskii S. et al., 2008, GCN 7482
Goodman J., MacFadyen A. I., 2007, preprint (arXiv:0706.1818)
Karpov S. et al., 2008, GCN 7558
Katz J., 1994, ApJ, 422, 248
Kennel C. F., Coroniti F. V., 1984, ApJ, 283, 694
Kumar P., McMahon E., 2008a, MNRAS, 384, 33
Kumar P., Panaitescu A., 2000a, ApJ, 541, L9
Kumar P., Panaitescu A., 2000b, ApJ, 541, L51
Kumar P., Panaitescu A., 2008, MNRAS, 391, L19
Larrabee D. A., Lovelace R. V. E., Romanova M. M., 2003, ApJ, 586, 72
Lazar A., Nakar E., Piran, 2009, preprint (arXiv:0901.1133)
Lithwick Y., Sari R., 2001, ApJ, 555, 540L
Lyutikov M., 2006a, MNRAS, 369, L5
Lyutikov M., 2006b, New J. Phys., 8, 110
Lyutikov M., Blandford R. D., 2003, preprint (astro-ph/0312347)
Medvedev M. V., 2000, ApJ, 540, 704
Mészáros P., 2002, ARA&A, 40, 137
Milosavljevic M., Nakar E., Zhang F., 2007, preprint (arXiv:0708.1588)
Narayan R., Kumar P., 2009, MNRAS, in press (arXiv:0812.0018)
Panaitescu A., Kumar P., 2002, ApJ, 571, 779
Piran T., 1999, Phys. Rep., 314, 575
Piran T., 2005, Rev. Mod. Phys., 76, 1143
Piran T., Shemi A., Narayan R., 1993, MNRAS, 263, 861
Racusin J. L. et al., 2008, Nat, 455, 183
Rees M. J., Meszaros P., 1994, ApJ, 430, L93
Rybicki G. B., Lightman A. P., 1979, Radiative Processes in Astrophysics. John Wiley & Sons, New York
Sari R., Piran T., 1997, ApJ, 485, 270
Sironi L., Goodman J., 2007, ApJ, 671, 1858

Thompson C., 1994, MNRAS, 270, 480
Thompson C., 2006, ApJ, 651, 333
Vreeswijk P. et al., 2008, GCN 7444
Wijers R. A. M. J., Galama T. J., 1999, ApJ, 523, 177
Wozniak P. R. et al., 2008, preprint (arXiv:0810.2481)
Zhang B., 2007, Chin. J. Astron. Astrophys., 7, 1
Zhang B., Kobayashi S., 2005, ApJ, 628, 315
Zou Y. C., Piran T., Sari R., 2009, preprint (arXiv:0812.0318)

APPENDIX A: POSSIBLE ERRORS IN THE CALCULATION OF IC FLUX

We discuss in this appendix possible sources of error in our calculation of the IC flux, i.e. errors associated with equation (48); according to this equation, the theoretically calculated gamma-ray flux is smaller than the observed value by a factor of $\sim$20.

A possible source of error might arise from our assumption of a homogeneous source, and we need to estimate its effect on the IC flux. The synchrotron peak flux is a linear function of magnetic field strength and the total number of electrons in the source, and therefore clumping of electrons and B, to lowest order, have little effect on the emergent flux. The IC flux is, however, affected by clumping of electrons, and we estimate the magnitude of this effect.

Let us consider an extreme form of inhomogeneity where all electrons are concentrated in $M_{\rm c}$ clumps of each size $r_{\rm c}$. The number density of electrons in the clumps is $n_{\rm c}$, and the density averaged over the source volume, $\sim R^3$, is n_0; there are no electrons in between clumps. Let us assume that the synchrotron power from each electron is p_ν. In this case, the synchrotron luminosity of the source is

$$L_{\rm syn}(\nu) \approx p_\nu (n_{\rm c} r_{\rm c}^3) M_{\rm c} \approx p_\nu n_0 R^3, \tag{A1}$$

and is independent of electron clumping. The IC luminosity depends on synchrotron flux in the vicinity of electrons (in clumps). The synchrotron flux is

$$f_{\rm syn}(\nu) \approx p_\nu (n_{\rm c} r_{\rm c} + n_0 R) \approx \frac{L_{\rm syn}(\nu)}{R^2}\left[1 + \frac{n_{\rm c} r_{\rm c}}{n_0 R}\right]. \tag{A2}$$

The IC luminosity is obtained from the above flux:

$$L_{\rm ic}(\nu_{\rm ic}) \approx \sigma_T f_{\rm syn}(\nu) n_{\rm c} r_{\rm c}^3 M_{\rm c} \approx \sigma_T L_{\rm syn}(\nu) n_0 R \left[1 + \frac{n_{\rm c} r_{\rm c}}{n_0 R}\right], \tag{A3}$$

or

$$L_{\rm ic}(\nu_{\rm ic}) \approx \sigma_T L_{\rm syn}(\nu) n_0 R \left[1 + f_{\rm c}^{-2/3} M_{\rm c}^{-1/3}\right], \tag{A4}$$

where $f_{\rm c} = n_{\rm c} r_{\rm c}^3 M_{\rm c}/(n_0 R^3)$ is the fraction of the shell volume occupied by clumps. We see from the above equation that IC flux can be enhanced by clumping of electrons. For instance, consider an example where $f_{\rm c} = 0.1$ and $M_{\rm c} = 1$ (all electrons are in a single small clump). The IC flux in this case is a factor of 4.5 larger than when electrons are uniformly distributed. This flux enhancement is about an order of magnitude smaller than what is needed to explain the observed flux for GRB 080319B (equation 48). An even more extreme case of clumping could bridge the gap, however the efficiency for converting jet energy to radiation is very small when $f_{\rm c} \ll 1$ as pointed out by Sari & Piran (1997). Furthermore, another serious problem is that a high degree of clumping leads to an increase of $\nu_{\rm a}$ (as discussed below), and that makes the SSC spectrum below the peak inconsistent with the observed data for GRB 080319B – unless we place the source at a distance from the centre of explosion that is larger than the deceleration radius.

The dependence of $f_{\rm ic}$ on $\eta \equiv \nu_i/\nu_{\rm a}$ is fairly strong and so we need to discuss the uncertainty in η. We have taken $\eta = 25$ ($\log \eta = 1.4$), which is guided by the Konus–Wind low-energy spectrum of $f_\nu \propto \nu^{0.2}$ in the energy band 20–650 keV. This low-energy spectral index suggests that $\nu_{\rm a}$ (the self-absorption frequency) should be $\lesssim$20 keV, and thus $\eta \gtrsim 32$; therefore, $\eta = 25$ is a conservative choice for GRB 080319B. However, is it possible that $\nu_{\rm a}$ has been overestimated in our calculation by our assumption of a homogeneous source? If $\nu_{\rm a}$ were to be smaller by a factor of $\sim$6 than given by equation (16) then that would lead to a larger IC flux by a factor of 30 (see equation 48), and thereby reconcile the observed and the theoretically expected gamma-ray flux. We show that inhomogeneities in the source cannot decrease $\nu_{\rm a}$ as long as the optical flux we observed during the burst is produced in the source.

We calculate synchrotron self-absorption frequency ($\nu_{\rm a}$) when B, γ_i and n_0 are allowed to vary, arbitrarily, across the source; the electron distribution is taken to be $\mathrm{d}n/\mathrm{d}\gamma = n_0(\gamma/\gamma_i)^{-p}$ for $\gamma \geq \gamma_i$. Spatial variations in B, γ_i and n_0 are subject to constraints that the optical flux and the IC peak frequency should be equal to the observed values.

Our starting point is equation (6.52) of Rybicki & Lightman (1979) for the synchrotron absorption coefficient, α_ν; $\int \mathrm{d}r' \alpha_\nu$ is the optical depth for absorbing synchrotron photons of frequency ν. We can show that for a power-law electron distribution and for $\nu < \nu_i$ (the case of interest for 080319B)

$$\alpha_{\nu'} \approx \frac{3^{1/2}(p+2)(p-1)q^3 n_0 B \sin\delta}{16\pi^2(p+2/3)m_{\rm e}\nu'^2\gamma_i}\left(\frac{\nu'}{\nu_i'}\right)^{1/3}, \tag{A5}$$

where

$$\nu_i' \equiv \frac{3qB\sin\delta\,\gamma_i^2}{4\pi m_{\rm e} c}, \tag{A6}$$

where δ is the angle between magnetic field and electron velocity vector, and prime denotes frequency in the source comoving frame. The synchrotron self-absorption frequency is determined from the equation

$$\int \mathrm{d}r'\,\alpha_{\nu'_\mathrm{a}} \approx \frac{3^{1/2}(p+2)(p-1)q^3}{16\pi^2(p+2/3)m_\mathrm{e}\nu'^2_\mathrm{a}} \int \mathrm{d}r'\,\frac{n_0 B\sin\delta}{\gamma_i}\left(\frac{\nu'_\mathrm{a}}{\nu'_i}\right)^{1/3} = 1, \tag{A7}$$

or

$$\nu'^{5/3}_\mathrm{a} \approx \frac{3^{1/2}(p+2)(p-1)q^3}{16\pi^2 m_\mathrm{e}(p+2/3)} \int \mathrm{d}r'\,\frac{n_0 B\sin\delta}{\nu'^{1/3}_i\gamma_i}. \tag{A8}$$

The ν'_a given by the above equation is self-absorption frequency along one line of sight. Since an observer receives photons from an area $\sim\pi R^2/\Gamma^2$, we should average ν_a over this area. This average frequency is given by

$$\langle\nu'^{5/3}_\mathrm{a}\rangle \approx \frac{3^{1/2}(p+2)(p-1)q^3}{16\pi^2 m_\mathrm{e}(p+2/3)}\frac{\Gamma^2}{\pi R^2}\int \mathrm{d}^3\boldsymbol{x}'\,\frac{n_0 B\sin\delta}{\nu'^{1/3}_i\gamma_i}. \tag{A9}$$

Since the optical flux (f_op) is proportional to $\int \mathrm{d}^3\boldsymbol{x}'\,n_0 B\sin\delta/\nu'^{1/3}_i$, when ν'_i lies above the optical band, it is convenient to define a new variable $\chi \equiv n_0\,B\sin\delta/\nu'^{1/3}_i$, and rewrite the equation for ν'_a using this new variable

$$\langle\nu'^{5/3}_\mathrm{a}\rangle \propto \frac{1}{R^2}\int \mathrm{d}^3\boldsymbol{x}'\,\frac{\chi}{\gamma_i}. \tag{A10}$$

The minimum of ν'_a can be obtained by requiring that $\delta\nu'_\mathrm{a} = 0$ for an infinitesimal variation of $\chi(\boldsymbol{x}')$, i.e.

$$\int \mathrm{d}^3\boldsymbol{x}'\,\frac{\delta\chi(\boldsymbol{x}')}{\gamma_i(\boldsymbol{x}')} = 0, \tag{A11}$$

subject to the condition that

$$\int \mathrm{d}^3\boldsymbol{x}'\,\delta\chi(\boldsymbol{x}') = 0. \tag{A12}$$

The variational integral implicitly assumes that we are solving for $\gamma_i(\boldsymbol{x}')$ which can be an arbitrary function as long as the IC spectral peak of the radiation emergent from the source matches the observed value, i.e. $1 \ll \gamma_i \ll \infty$. Let us consider a special form of $\delta\chi(\boldsymbol{x}')$ that is non-zero in two spherical regions of infinitesimal radius centred at $\boldsymbol{x}'_1$ and $\boldsymbol{x}'_2$. It is required that $\delta\chi(\boldsymbol{x}'_1) = -\,\delta\chi(\boldsymbol{x}'_2)$ in order to satisfy the optical flux constraint. Substituting this into equation (A11) leads to $\gamma_i(\boldsymbol{x}'_1) = \gamma_i(\boldsymbol{x}'_2)$. Since, $\boldsymbol{x}'_1$ and $\boldsymbol{x}'_2$ were arbitrary points in the source, we conclude that γ_i does not vary across the source when ν'_a is minimized. Therefore, we can take γ_i outside of the integral in equation (A10), and find that the minimum value of $\langle\nu_\mathrm{a}\rangle$ is fixed by the observed optical flux. In other words, the assumption of a homogeneous source used in our calculations in Sections 3 and 4 gives the smallest possible value for η or the largest IC flux. For a high degree of clumping of electrons in the source, we considered above, ν_a is larger when our line of sight passes through a clump and especially when only one clump lies on our sight line; there is, however, little change to $\langle\nu_\mathrm{a}\rangle$ as we have shown above. In this case, an observer will receive radiation from one clump at a time, and will find ν_a larger than the case of a homogeneous shell. A larger ν_a for a clumpy source goes in the opposite direction to what we need to increase the IC flux, and this largely reverses the gain to the IC flux found above (equation A4).

We assumed in our derivation that ν'_i is above the optical band. A similar proof for the minimum of ν'_a can be carried out when ν'_i is below the optical frequency. Moreover, we ignored variations of Γ across the source. This approximation is justified since large variation in Γ are smoothed out in less than one dynamical time.

There is one effect that we have not included in our calculation which lowers the value of the self-absorption frequency ν_a somewhat. As synchrotron photons propagate outwards they move though a medium where the electron density is decreasing with time (due to the outward expansion of the shell). As a result, a calculation based on a stationary source overestimates the optical depth to Thomson scattering and ν_a by factors of $\sim$2 and $\sim 2^{3/5}$, respectively. This can be seen by considering a homogeneous shell with electron density n_0 located at a distance R_0 from the centre of explosion, with a radial thickness R_0/Γ^2. (The comoving frame shell thickness of R_0/Γ is obtained by causality considerations, since $R_0/c\Gamma$ is the time elapsed in the shell comoving frame.) As seen by a lab frame observer, a photon moving outwards in the radial direction takes a time $2R_0/c$ to cross the shell, and during this time the shell has moved to a larger radius and the density has decreased. For a hot shell, the radial width too increases with time, and the photon transit time is a bit larger still. A straightforward calculation of the optical depth to Thomson scattering when the density changes as $1/R^2$ shows that the shell optical depth is about half of what it is for a stationary medium of the same thickness and density. Substituting this optical depth into equation (A8) for ν_a we see that the synchrotron-self absorption frequency is smaller for an expanding shell by a factor of $\sim 2^{3/5}$.

The net effect is that the parameter η which is defined in equation (17) should be reduced by a factor of $2^{3/5}$. In the case of GRB 080319B, we estimated $\eta \sim 25$ from the observations. We should use a smaller value $\eta \sim 16$ in our formulae to obtain more accurate numerical estimates of quantities. This causes the predicted gamma-ray flux to be increased by a factor of 2.5.

This paper has been typeset from a TEX/LATEX file prepared by the author.